Elsevier Editorial System(tm) for Quaternary Science Reviews

Manuscript Draft

Manuscript Number:

Title: The Valle di Manche section (Calabria, Southern Italy): a high resolution record of the Early-Middle Pleistocene transition (MIS 21-MIS 19) in the Central Mediterranean

Article Type: Research paper

Keywords: Early/Middle Pleistocene; MIS 19; Southern Italy; Crotone Basin; GSSP; chronostratigraphy

Corresponding Author: Dr. Luca Capraro,

Corresponding Author's Institution: University of Padova

First Author: Luca Capraro

Order of Authors: Luca Capraro; Patrizia Ferretti; Patrizia Macrì; Daniele Scarponi; Fabio Tateo; Eliana Fornaciari; Giulia Bellini; Giorgia Dalan

Abstract: The on-land marine Valle di Manche section (Crotone Basin, Calabria, Southern Italy) is one of the candidates to host the GSSP of the Middle Pleistocene ("Ionian") Stage. The section preserves an excellent record of the Matuyama-Brunhes magnetic reversal, which occurs in the midst of Marine Isotope Stage (MIS) 19, along with a wide set of independent chronological, paleoclimatic and stratigraphic proxies, which permit a straightforward correlation with marine and terrestrial reference records at the global scale. We have recently started a complete revision of the section, which provides a dramatic improvement to our knowledge of the section especially in the stratigraphic interval close to the Lower-Middle Pleistocene boundary. The benthic δ18O record provides evidence that in the Valle di Manche section the Matuyama-Brunhes transition occurred during full MIS 19, in agreement with most of the available records worldwide. Its stratigraphic position is marked by a prominent tephra (the "Pitagora ash"). We have achieved the age of 786.9 ka for the Matuyama-Brunhes magnetic reversal and pinpointed the paleomagnetic transition of to a 3 cm-thick interval, indicating that the event was very fast. Since the section fulfills all the requirements to host the GSSP of the Ionian Stage, we propose that the boundary should be placed at the base of the "Pitagora ash", ca. 12.5 cm below the midpoint of the Matuyama-Brunhes reversal.

Suggested Reviewers: Biagio Giaccio
Researcher, Istituto di Geologia Ambientale e Geoingegneria, CNR, Rome, Italy
biagio.giaccio@cnr.it
Expert in Quaternary geology, tephrostratigraphy and paleoclimatology

Brad Pillans
Professor, Research School of Earth Sciences, Australian National University
brad.pillans@anu.edu.au

Expert in Quaternary geology and chronostratigraphy

Giovanni Zanchetta
Associate Professor, Dipartimento di Scienze della Terra, University of Pisa, Italy
zanchetta@dst.unipi.it
Geochemist specifically committed to the study of stable oxygen isotopes of the Quaternary

lunedì 29 agosto 2016

The Valle di Manche section (Calabria, Southern Italy): a high resolution record of the Early-Middle Pleistocene transition (MIS 21-MIS 19) in the Central Mediterranean

Luca Capraro[1#], Patrizia Ferretti[2], Patrizia Macrì[3], Daniele Scarponi[4], Fabio Tateo[5], Eliana Fornaciari[1], Giulia Bellini[1], Giorgia Dalan[1]

[1] Dipartimento di Geoscienze, University of Padova, Via G. Gradenigo 6, I-35131 Padova, Italy

[2] CNR-IDPA, Via Torino 155, I-30172, Venezia Mestre, Italy

[3] Istituto Nazionale di Geofisica e Vulcanologia, Via di Vigna Murata 605, I-00143 Roma, Italy

[4] Dipartimento di Scienze Biologiche, Geologiche e Ambientali, University of Bologna, via Selmi 3, I-40126 Bologna, Italy

[5] CNR-IGG, Via G. Gradenigo 6, I-35131 Padova, Italy

Corresponding Author: luca.capraro@unipd.it

1 – Introduction

The definition of Global Stratotype Sections and Points (GSSPs) is one of the main tasks to be accomplished by the Earth scientists' community. The recognition of formal boundaries and chronostratigraphic units represents indeed a fundamental step towards a common language in stratigraphy, which is of the essence for the future work.

So far, the Pleistocene Series is subdivided into 4 Stages, two of which (Gelasian and Calabrian, Lower Pleistocene) have only been formally defined (Rio *et al*., 1998; Cita *et al*., 2012). The "Ionian" and "Tarentian" Stages (Middle and Upper Pleistocene, respectively) are employed informally,

though their definition is expected shortly.

In keep with all Pliocene and Pleistocene Stages, there is a large agreement to define the GSSP of the Ionian Stage in correspondence to a paleomagnetic event, namely the Matuyama-Brunhes reversal, in mid-MIS 19 (Richmond, 1996; Head *et al.*, 2008; Pillans and Gibbard, 2012). Unfortunately, the Matuyama-Brunhes (M-B) boundary is usually poorly documented in the marine on-land record (Singer, 2014). To our knowledge, the only available marine on-land record of the M-B reversal in the Mediterranean area is that of the Valle di Manche section (VdM hereafter), located in the Crotone sedimentary basin (Calabria, Southern Italy).

The VdM section was investigated since the early 1990s (Rio *et al.*, 1996; Capraro *et al.*, 2005). However, the amount and resolution of the data published so far is nowadays inadequate, considering the recent trend towards high-resolution studies. Hence, we recently undertook a complete revision of the local succession in order to obtain a more detailed and complete information on the VdM section, with the aim of supporting a formal proposal of definition of the GSSP of the Ionian Stage (Cita *et al*., 2006).

Based on the new data, we will demonstrate that the VdM section holds all the key requirements for the definition of a GSSP, as per the recommendations of Remane *et al.* (1996).

Given that all GSSPs of the Pliocene and Pleistocene Series ratified so far are located in the Crotone Basin and Sicily, defining the GSSP of the Ionian Stage in the VdM section would also comply to a basic principle of regional and historical continuity, with understandable benefits (high correlation potential, comparable depositional settings and proxies, simple logistics, etc.).

2 – Geologic setting

The Neogene Crotone sedimentary basin (Calabria, Southern Italy; Fig. 1) hosts an exceptionally thick

and well-exposed succession of highly fossiliferous upper Miocene to Pleistocene marine sediments. The Crotone Basin is interpreted as a forearc basin located above the internal part of the Calabrian accretionary wedge (Rossi and Sartori, 1981; Barone *et al.*, 1982; Van Dijk and Okkes, 1991). The sedimentary succession of the Crotone Basin was subdivided by Roda (1964) into three tectono-stratigraphic sequences bounded by major unconformities, which point to episodes of deformation and basin reorganization (Massari *et al.*, 2010; Macrì *et al.*, 2014). The youngest sequence was prompted by a sharp increase in the regional subsidence rates during the Piacenzian, which led to the basinwide deposition of monotonous open-marine muds (the "Cutro" marly clays of Rio *et al*., 1996). In a large part of the basin, the "Cutro" marly clays are truncated and overlain directly by Middle to Upper Pleistocene marine terrace deposits, in response to the regional uplift that commenced during the Calabrian (Massari *et al.*, 2010; Capraro *et al.*, 2011).

In confined sectors of the Crotone Basin, such as the San Mauro area, tectonic subsidence promoted the development of small sub-basins, where marine sedimentation lasted longer (Rio *et al.,* 1996; Massari *et al.*, 2010; Capraro *et al.*, 2011; Macrì *et al*., 2014).

2.1 - The San Mauro sub-basin

The San Mauro sub-basin is located in the internal part of the Crotone Basin (Fig. 1). It is bounded by two northeast–trending dextral oblique-slip faults (Rio *et al.*, 1996; Massari *et al.*, 1999) that became active during the Early Pleistocene (Massari *et al.*, 2002) and promoted the growth of a synsedimentary syncline, where a shallowing-upward, marine to continental succession was laid (the "San Mauro Sandstone" of Rio *et al.*, 1996; SMS hereafter).

The SMS, composed of a stack of nine transgressive/regressive (T/R) cycles that reflect the local sedimentary response to changes in sea level and sediment supply (Massari *et al*., 2002, 2007; Capraro *et al.*, 2005), was subdivided by Rio *et al.* (1996) into three sub-units (SM1 to SM3; Fig. 1)

that can be traced across the San Mauro sub-basin.

The basal SM1 unit consists of a distinctive prograding package of shallow-water, coarse-grained sands that attain to a maximum thickness of ca. 45 m (Massari *et al.*, 2002). Shells of the boreal guest *Arctica islandica* are locally common. The micropaleontological content is distinctively poor, being represented by reworked calcareous microfossils and shallow-water benthic foraminifers (Rio *et al.*, 1996). The SM1 unit rests unconformably on top of the "Cutro" marly clays, which are truncated above the Base of *Gephyrocapsa* sp.3 (*sensu* Rio, 1982), calibrated with MIS 25 in the Central Mediterranean (Castradori, 1993; Raffi *et al.*, 2006). Capraro *et al.* (2005) confirmed that the SM1 unit correlates to the MIS 24-22 glaciation.

The SM2 unit, ca. 5 to 40 m thick, is represented by a prominent grayish package of soft outer- to mid-shelf deposits, ranging from silty muds to sandy silts. The SM2 unit spans from the uppermost MIS 22 to the MIS 18.4 glacial (Capraro *et al.*, 2005). Stratal geometries and thicknesses (Massari *et al.*, 2002, 2007, 2010) point to a significant deepening and increase of the local tectonic subsidence rates at the demise of the MIS 24/22 glaciation, which emphasized dramatically the effects of glacioeustasy (Capraro *et al.*, 2005). The SM2 muds contain a prominent, sharp-based tephra layer (Rio et al., 1996), the "Pitagora ash". It contains a substantial volcaniclastic fraction made of glass shards and magmatic crystals. Its thickness is variable, ranging from ca. 3-4 cm in marginal settings, where the crystal size is coarser, to 30 cm in depocentral areas, where the fine (silty) fraction is dominant (Rio *et al.*, 1996). The "Pitagora ash" can be traced easily basinwide, and represents the most practical and reliable tool for long-distance correlations within the San Mauro sub-basin (Rio *et al.*, 1996). Indeed, the "Pitagora ash" provides unambiguous physical linkage between depocentral sections – where the stratigraphic architecture is basically represented by a mere vertical stack of T/R cycles – and marginal areas, where sedimentary bodies are often amalgamated and truncations, omission surfaces and facies changes are widespread (Massari *et al.*, 2002, 2007).

The SM3 unit, attaining to a total thickness of ca. 120 m in depocentral areas (Massari *et al.*, 2002), is composed by a basal siciliclastic prograding shallow-water sandy body, locally very rich in bivalve shells, that grade upwards into a complicated alternation between fluvial gravels, sands and lagoonal muds. It represents the youngest infill of the San Mauro sub-basin (i.e., post-MIS 18) prior to the uplift of the area (late Middle Pleistocene; Capraro *et al.*, 2011).

3 – The section

The VdM section is well exposed along the northwestern flank of the Manche valley, just below the cemetery of the village of San Mauro Marchesato (Fig. 1). Access to the outcrop is free and easy. It preserves the most continuous, expanded and undisturbed record available of the SMS (Rio *et al.*, 1996; Massari *et al.*, 2002; Capraro *et al.*, 2005).

The VdM section was laid in a depocentral setting of the San Mauro sub-basin (Massari *et al.*, 2002) where, in contrast with the marginal (landward) areas, transgressive-regressive cycles are separated by conformable surfaces and the stratigraphic record is complete (Rio *et al.*, 1996; Massari *et al.*, 2002, 2007).

3.1 – Materials and methods

We pinpointed the razor-sharp base of “Pitagora ash”, which represents the most distinctive horizon of the section, as the zero-elevation surface.

One meter at a time, we removed the regolith and described the physical stratigraphy of a fresh, smooth surface of the bedrock. To this effect, we employed an emended version (Tab. 1) of the facies description proposed in Capraro *et al.* (2005), to which we refer for further details.

Afterwards, blocks of ca. 300 g of sediment were collected at a regular stratigraphic distance of 25 cm. Exceptions were made in the critical interval straddling the “Pitagora ash”, where sampling

resolution was much higher (up to ca. 2 cm), and in the layered silty unit, where we picked a sample from any individual stratum (ca. 20 cm/sample).

The sampled interval is ca. 37 m thick. In the well exposed interval above the "Pitagora ash" (SMA samples; Fig. 2) we extended our investigation up to ca. 13.5 m level (sample SMA 56; Fig. 2), at the bottom of the sandy SM3 unit (Rio *et al.*, 1996; Capraro *et al.*, 2005).

Below the "Pitagora ash", we followed the same trajectory as above for a stratigraphic distance of ca. 3 m (samples SMA-1 to SMA-14 in Fig. 2), where a small patch of vegetation forced us to move horizontally by ca. 2.5 m and to proceed along a contiguous profile. Relocation was safe, because we exploited the marker bed rich in *Turritella tricarinata* that can be traced easily across the VdM badland. For the sake of information, samples were coded SMB afterwards. We halted our investigation at the -23.25 m level (sample SMB 76), at the top of the shallow-water SM1 sands (MIS 22; Fig. 2).

Samples were dispatched to the Department of Geosciences of the University of Padova, where they were dried, weighted and then split into smaller fragments. Ca. 100 g of sediment were washed for the analysis of foraminifer content; smaller quantities (40 g and 10 g) were processed for the study of pollen and calcareous nannofossils, respectively. The remains were sealed into small plastic bags and stored conveniently in the Department's warehouse for future use and reference.

3.2 – Results

The reconstructed stratigraphic log (Fig. 2) shows a closely spaced, yet consistent, alternation of facies. We emphasized graphically the lithological contrasts and boundaries only with the aim of stressing the well-developed stratigraphic architecture of the section. We insist that, as anticipated by Massari *et al.* (2002, 2007), facies changes at VdM are very subtle, always gradual, and no evidence occurs of erosional surfaces, hiatuses, variations in sediment composition and/or abrupt

changes in the sedimentation style, which is persistently dominated by mud settling (Massari *et al.,* 2002, 2007).

The depositional setting at VdM ranges from middle shelf to outer shelf/upper slope, in full agreement with the coeval stratigraphy at the Montalbano Jonico section (D'Alessandro *et al.*, 2003; Stefanelli, 2003). In contrast with the latter, which is mainly represented by a monotonous succession of hemipelagic muds, changes in the local sea-level at VdM result in an articulated stacking pattern of facies that represents a significant bonus, because it provides a solid validation of the independent proxies of sea-level such as the $\delta^{18}O$ curve and the mollusk faunas.

The stratigraphic architecture of the SM2 at VdM permits the firm recognition of two T/R cycles, which resulted from a close interplay between glacieustasy, sediment yield and tectonics. Repetitive patterns in the stacking of facies point to the persistence of similar depositional conditions during the sedimentation of each T/R cycle, suggesting that the main traits of the VdM succession were primarily shaped by glacioeustasy. Superimposed is a strong local subsidence, which promoted the continuous creation of accommodation space and the persistence of open marine conditions, with deposition of a continuous and expanded stratigraphic succession.

4 – Stable Oxygen Isotopes

We have reconstructed a continuous $\delta^{18}O$ stratigraphy for the infaunal benthic foraminiferal species *Uvigerina peregrina* (Fig. 2), which has long been demonstrated to precipitate its calcite in oxygen isotopic equilibrium with respect to seawater (Shackleton, 1974). The $\delta^{18}O$ of this species represents the best practical tool for correlation to the open marine records at a global extent, as it holds a strong glacioeustatic component during the time interval considered in this study (Shackleton, 1974; Elderfield *et al*., 2012).

4.1 – Materials and methods

For stable isotope analyses, 143 rock samples were washed on a 63-µm sieve using distilled water, oven-dried on the sieves at 50°C, and then weighed. From the fraction >150 µm we hand-picked pristine specimens of *U. peregrina*, which is generally well preserved and occur continuously throughout the interval analyzed in this study.

Between 10 and 15 specimens were employed for each isotopic analysis. Tests were gently crushed under the microscope using two clean glass plates, transferred to the mass-spectometer vials and soaked in 3% hydrogen peroxide, in order to remove any possible organic contaminant. Analytical grade acetone was then added and samples were cleaned ultrasonically, after which the excess liquid was siphoned off. The samples were finally dried in an oven at 50°C before the analysis.

Carbon dioxide for isotopic analysis was released using orthophosphoric acid at 70°C in an automated continuous flow carbonate preparation GasBench II device, and analysed in a Thermo Scientific Delta V Advantage Isotope Ratio Mass Spectrometer at the Department of Geosciences of the University of Padova. The laboratory standard (Carrara marble MAQ1) was calibrated to VPDB through NBS 19, using the values of -2.20‰ for the $\delta^{18}O$ and +1.95‰ for the $\delta^{13}C$, as recommended by Coplen (1988, 1994). Analytical reproducibility (as indicated by the MAQ1 analyses) was ±0.09% (1σ).

4.2 – Results

The benthic $\delta^{18}O$ values range from 1.62 to 4.34‰ VPDB (Fig. 2). The “lightest” (interglacial) values are in good agreement with the isotopic compositions of modern *Uvigerina* spp. in the eastern Mediterranean basin, ranging from 1.80‰ in the Sicilian Strait to 2.20‰ in the Levantine Sea (Vergnaud Grazzini *et al.*, 1986). Likewise, “heavier” (glacial) values compare well to those calculated

for *Uvigerina* spp. from various water masses during the Last Glacial Maximum (4.9‰ to 4.25‰; Vergnaud Grazzini *et al.*, 1986). This correspondence is positively surprising, because it is usually assumed that the isotopic signal in a shelf setting may be heavily disturbed by local factors, such as temperatures and river runoff, and not correlate to the open marine records.

A simple visual correlation of our $\delta^{18}O$ stratigraphy to open marine reference records (e.g., Lourens, 2004; Lisiecki and Raymo, 2005) confirms that the studied interval spans continuously from the termination of MIS 22 to full MIS 18.4.

In spite of the increased sampling resolution with respect to that available in Capraro *et al.* (2005), information is still poor in the condensed interval corresponding to MIS 21. In contrast, the glacial termination of MIS 20 (i.e., the MIS 20-MIS 19 transition) is very expanded, attaining to the remarkable thickness of ca. 10 m.

5 – Chronology

An essential prerequisite in reconstructing a robust age model is the choice of an appropriate tuning target. As a common practice, individual isotope records worldwide are usually tuned via the comparison to benthic $\delta^{18}O$ deep-water North Atlantic successions, in spite of their geographic location. However, oceanographic differences between the studied area and the North Atlantic region may be vast (e.g., Suganuma *et al.*, 2015) and potentially misleading. Therefore, the most suitable tuning target should be chosen taking into account the local depositional setting and circulation systems, as well as the regional evapotranspiration and temperature budgets.

5.1 – Present-day oceanographic setting

The Crotone Basin is presently located at the north-western margin of the Ionian Sea (central-eastern Mediterranean). The Mediterranean is a landlocked concentration basin, where

evapotranspiration exceeds the freshwater input provided by river runoff and precipitation (e.g., Tanhua *et al.*, 2013). The regional interplay between regional freshwater and heat budgets promotes an anti-estuarine thermohaline circulation at the basin scale, resulting in a surface inflow through the straits of Gibraltar and a congruent deep-water outflow (Bethoux *et al.*, 1992). The Atlantic Waters (AW) enter the Mediterranean and rapidly evolve to Modified Atlantic Waters (MAW), which are constrained to a ca. 200 m-thick surface layer flowing eastward. In the course of their path across the basin, the MAW experience a gradual increase in temperature and salinity (Wüst, 1961; Malanotte-Rizzoli and Hecht, 1988). During the winter season, cold northern winds cause heat loss and vertical convection, that eventually results in sinking of the MAW and enucleation of the Levantine Intermediate Waters (LIW; Malanotte-Rizzoli and Hecht, 1988; Lascaratos *et al.*, 1993) that flow westward at a depth between 200 and 600 m, persistently below the MAW (Borzelli et al, 2009; Gačić *et al.*, 2011; Bensi *et al.*, 2013).

The present-day circulation of the upper thermocline in the Central Mediterranean (Ionian Sea) is exerted by jets, meandering currents and gyres that develop within the MAW (Malanotte-Rizzoli and Bergamasco, 1991; Robinson *et al.*, 1991; Malanotte-Rizzoli *et al.*, 1999, 2014). After crossing the Sicilian Sill (Fig. 3), the MAW enter the Ionian Basin conveyed by the Atlantic-Ionian Stream (AIS; Malanotte-Rizzoli *et al.*, 1997). The AIS follows a meandering path protruding northeastward, and then splits into two major branches: one flows southward and enters the Ionian Anticyclone (IA), the other first extends northward and then curves abruptly southeastward, after grazing the Crotone peninsula (Fig. 3).

The isotopic composition of surface waters in the Ionian Sea is consistent, with minor variations at the basin scale (Pierre, 1999). Indeed, surface waters offshore the Crotone peninsula do not differ significantly, in terms of temperature and salinity, from those of the open Ionian Sea (Malanotte-Rizzoli *et al.*, 1997). By contrast, composition of the MAW (Pierre, 1999) is very different from that of

their original source, namely the surface waters flowing through Gibraltar from the North Atlantic (Frew *et al.*, 2000). Consequently, correlation to the North Atlantic $\delta^{18}O$ records should be approached very carefully, even in the case of isotopic records reconstructed in adjacent and interconnected basins.

5.2 – Methods

Well-dated Mediterranean $\delta^{18}O$ records straddling the MIS 21-MIS 19 interval are very few and solely based on planktic species (Lourens, 2004). Among these is the KC01b core, recovered in the central Ionian Sea (Castradori, 1993; Lourens, 2004) that, other than representing a pristine documentation of the regional $\delta^{18}O$ stratigraphy, was astronomically tuned and compared to the open ocean successions (Lourens, 2004).

The benthic $\delta^{18}O$ curve of *U. peregrina* at VdM shows a striking likeliness with the $\delta^{18}O$ record of *G. ruber* reconstructed for the KC01b core, suggesting that they reflect similar seawater properties (Fig. 4). Indeed, the estimated water depth at which the VdM succession was laid extends from ca. 60 to 150 m (Scarponi *et al.*, 2014), well into the range at which the MAW reside and significantly shallower than the benthic open-ocean records. We can reasonably assume that the isotopic events documented by the benthic $\delta^{18}O$ record at VdM are synchronous and similar in amplitude to those recorded by the planktonic $\delta^{18}O$ KC01b record, aside from local influences – such as riverine input – and different isotope fractionation of seawater by the analyzed foraminifer species.

In order to minimize the influence of local effects, we employed as target the Mediterranean isotopic Stack of Lourens (2004), a merger of individual planktonic $\delta^{18}O$ records recovered from the central Ionian (core KC01b) and Levantine basins (ODP Site 976). The shape of the Mediterranean Stack is very close to that of the KC01b core alone, suggesting that the isotopic composition of surface waters in the Eastern Mediterranean is similar at the regional scale (Pierre, 1999).

We identified 11 control points (Fig. 4; Tab. 2) that provide a tight linkage between the VdM $\delta^{18}O$ record and the Mediterranean Stack. Age of the intervening data points is calculated by a simple linear interpolation. Tie points were chosen at the mid-points of the glacial terminations of MIS 21 and 19 (866 and 794 ka, respectively) and in correspondence to conspicuous maxima and minima (peaks) of the isotopic curves. In the VdM curve, we did only consider as reliable all the $\delta^{18}O$ peaks generated by 3 data points at least, while we discarded those represented by a single value. During the process, we carefully and continuously checked the resulting sediment accumulation rates, in order to reconstruct an age model consistent with the physical stratigraphy of the section and with the average sedimentation rates calculated for the Pleistocene successions of the Crotone Basin.

5.4 – Results

According to our reconstruction, the studied record spans from ca. 740 to 870 ka. The proposed age model is consistent with the expected chronology and respectful of the initial conditions. Indeed, the VdM record is virtually not stretched or deformed in the critical MIS 20-MIS 18 interval with respect to the original stratigraphy (Fig. 2), suggesting that our age model is robust across MIS 19.

5.4.1 - Sediment accumulation rates

The estimated sediment accumulation rates provide a simple yet valuable gauge of the robustness of an age model. Being calculated by linear interpolation, they change accordingly to the stratigraphic position of control points and their putative age. However, sediment accumulation rates must be coherent with the local depositional setting, and they should vary significantly only in correspondence to a congruent change in the physical stratigraphic framework.

The sediment accumulation rates calculated for the VdM section (Tab. 1) range from a minimum of ca. 5 cm/kyr to a maximum of ca. 94 cm/kyr. As expected, relative minima characterize the fine-

grained intervals corresponding to the interglacials of MIS 21 and MIS 19 (5 and 27 cm/kyr, respectively). In contrast, sedimentation velocity increased during the MIS 20 glacial (up to ca. 42 cm/kyr) and during the MIS 22-MIS 21 and MIS 20-MIS 19 transitions (58 and 94 cm/kyr, respectively). The unusual stratigraphic expansion at the glacial termination of MIS 20 was discussed and explained by Massari *et al.* (2007), to whom we refer for further details.

In the critical full MIS 19 interval, i.e. across the M-B boundary, the average sediment accumulation rates are in the order of ca. 27 cm/kyr, significantly higher than those (ca. 13 cm/kyr) proposed by Capraro *et al.* (2005) but perfectly in agreement with those reported for many shelfal Pleistocene sections of the Crotone Basin (Capraro *et al.*, 2011).

In general, sediment accumulation rates at VdM change in keep with both the physical stratigraphy and the local $\delta^{18}O$ curve, pointing to a strong glacioeustatic forcing on sedimentation. Occasionally, eustasy was probably outpaced by sediment yield to the basin margin in response to severe climatic conditions and/or local subsidence, such as during the MIS 20-MIS 19 transition (Massari *et al.*, 2007).

5.4.2 – Paleodepth of the VdM section

According to Scarponi *et al.* (2014), the local paleodepths varied from ca. 60 to 150 m with a minimum of ca. 25-30 m in the SM1 unit (MIS 24/22), which was not investigated for this work.

Being a sound proxy of the global sea-level (Shackleton, 1967), the $\delta^{18}O$ record of *U. peregrina* represents a benchmark for testing the paleodepth curve reconstructed by Scarponi *et al.* (2014) based on the fossil mollusk fauna. The correlation is excellent (Fig. 5) and provides an independent proof that, in spite of the shelfal setting, the $\delta^{18}O$ record of *U. peregrina* essentially preserves a glacioeustatic component.

The "lightest" $\delta^{18}O$ values of *U. peregrina* point to the Maximum Eustatic (=global) Depth (MED) of MIS 21 and MIS 19. The latter precede the Local Maximum Depth (LMD) horizons, which are marked by sediment starvation and the development of firmgrounds rich in *Neopycnodonte cochlear* (Facies B in Fig. 2). Based on the sediment accumulation rates calculated for the interglacial maxima of MIS 21 and 19 (10 and 27 cm/kyr, respectively), the LMD is likely to lag behind the MED by ca. 5 kyr. We speculate that this significant time lag reflects the strong local subsidence that, in the VdM area, persisted in creating accommodation space, and therefore deepening, well after the end of the eustatic transgression.

6 – Calcareous nannofossils

The chronostratigraphic interval between late MIS 25 and late MIS 16 (from ca. +0.9 to ca. +0.6 Ma), which includes the VdM record, is especially difficult to assess by means of a conventional marine biostratigraphy. Indeed, calcareous nannofossil assemblages show no significant evolutionary changes in the Central Mediterranean basin between the Base common (Bc) of calcareous nannofossil *Gephyrocapsa* sp.3/*omega* (*sensu* Rio, 1982), calibrated with MIS 25 (base of the "*Pseudoemiliania lacunosa*" Zone, ca. 950 ka; Castradori, 1993) and the Top (T) of the species (MIS 15; Raffi *et al.*, 2006). However, this interval is marked both by episodes of temporary appearance/disappearance and fluctuations in the relative abundance of different species within the genus *Gephyrocapsa*. These events occur at the regional scale and probably reflect physical and chemical changes in the photic zone, being consistent with the milankovian (glacial/interglacial) climate variability (e.g., Raffi *et al.*, 2006).

6.2 – Materials and methods

For the analysis of calcareous nannofossil assemblages, we investigated 74 samples in the interval

between MIS 21 and the MIS 19-MIS 18 transition. For each sample, a small fragment of dry sediment was ground onto a cover slip, moistened with a drop of distilled water and smeared across the cover slip with a wooden tooth pick. The cover slip was then glued to a slide using Norland optical adhesive cured under U.V. light.

Single slides were examined using a light microscope at the 1250x magnification. Investigation was performed following a semiquantitive method, namely counting the number of specimens belonging to the genus *Gephyrocapsa* (different species) within a smearslide area of ca. 1 mm^2 (Backman and Shackleton, 1983). We estimated the relative abundances of *G.* sp.3/*omega*, *G. oceanica* and *G. caribbeanica* (Fig. 6), which allowed the recognition of eco-biostratigraphic intervals (Ecozones) largely validated for the central Mediterranean area (e.g., Maiorano and Marino, 2004; Raffi *et al.*, 2006).

6.3 – Results

Indigenous calcareous nannofossils are present with variable abundances throughout the studied interval, with highest concentrations and best preservation in the fine-grained intervals corresponding to full MIS 21 and MIS 19. The distribution pattern of the total gephyrocapsids assemblage shows a striking resemblance with the $\delta^{18}O$ record of U. peregrina, with peaks of abundance centered on the LMD intervals of MIS 21 and MIS 19 (Fig. 6.a).

Gephyrocapsa sp.3/*omega* reflects conditions of warm, nutrient-rich surface waters and low salinity (Maiorano and Marino, 2004). Indeed, the species is very common during interglacial periods and rare to absent during glacial intervals. However, long records from the central Mediterranean (e.g., Castradori, 1993; Maiorano and Marino, 2004) demonstrate that *G.* sp.3/*omega* is extremely scarce during the MIS 19 interglacial, being conversely very common in the contiguous MIS 21 and 17. This distribution, already well documented in other sections of the Crotone Basin (Capraro *et al.*, 2011), is

for the first time recognized unambiguously in the VdM section (Fig. 6.c).

Gephyrocapsa oceanica is reported to thrive in ecological conditions similar to those suggested for *G.* sp.3/*omega* (e.g., Thierstein *et al.*, 1997; Flores *et al.*, 1999, Sprovieri *et al.*, 2003; Melinte, 2005). Indeed, interglacial MIS 21 and MIS 19 in the VdM section are also characterized by the dominance of warmth-demanding foraminifer species, among which the surface dweller *Globigerinoides ruber*, indicative of warm, oligotrophic and well-stratified waters (Pujol and Vergnaud Grazzini, 1995), is prevalent. The MIS 19 interglacial in the VdM section is dominated by *G. oceanica* (predominantly represented by specimens ≥ 4 µm in size; Fig. 6.b), in keep with what reported by Sprovieri *et al.* (1998) for the Sicilian Strait.

The species *G. caribbeanica* is considered indicative of cool to cold surface waters (e.g., Wells and Okada, 1996, 1997; Flores *et al.*, 1999; Villa *et al.*, 2005), which are reasonably correlated to glacial intervals. Being the species confined to glacial events and their terminations (Fig. 6.d), its distribution pattern in the VdM section seems to confirm its preference for cool/cold waters. An excellent documentation is provided by the expanded termination of MIS 20, where the deep-dwelling *Globorotalia inflata*, indicative of a persistently cold, vertically mixed water column (Pujol and Vergnaud Grazzini, 1995; Hemleben *et al.*, 1989) is very abundant (Capraro *et al.*, 2005).

Regrettably, it was not possible to detect the T of *Reticulofenestra asanoi*, which would occur within the upper MIS 22 sands (Raffi *et al.*, 2006), where nannofossils are only represented by a reworked assemblage (Rio *et al.*, 1996).

We also accomplished a qualitative evaluation of the amount of reworked nannofossils with respect to the total indigenous assemblage (Fig. 6.e). As expected, the maximum input of displaced material correlates to $\delta^{18}O$ glacial intervals (MIS 22, MIS 20, MIS 18.4), characterized by low sea level and massive sediment yield to the basin. In contrast, a native nannofossil population is dominant during interglacial periods, when the terrestrial sources of terrigenous input were farthest from the

sedimentation area.

7 – Pollen

The pollen record of the VdM section provides useful insights on the evolution of natural landscapes in the Crotone area in response to changes in global and regional climates. It reflects a logical succession of vegetation states in excellent agreement with the $\delta^{18}O$ record, as demonstrated by previous low-resolution analyses (Capraro *et al.*, 2005, 2006). We focused our investigation on the interval straddling the MIS 19 interglacial only, which is now documented with a much higher resolution than that previously available (Capraro *et al.*, 2005).

7.1 – Materials and methods

We analyzed 46 samples in the interval between -3.75 and +7.06 m (samples SMB2 to SMA30), which covers the whole MIS 19 interglacial (Fig. 7). Notably, this very interval was previously represented by 17 samples only (Capraro *et al.*, 2005). 10 grams of oven-dried sediment were treated following the standard techniques for samples preparation for palynological analyses (HCl, HF, gravitative separation via heavy liquids, ultrasound treatment) modified according to our internal lab procedures. Samples were mounted on disposable slides by means of glycerin jelly, and observed at the optical microscope with a maximum magnification of 640x.

Following a common practice, *Pinus* was excluded from the statistical analysis, as well as dinoflagellate cysts and fungal and fern spores. A minimum of 200 pollen grains (*Pinus* excluded) were counted for each sample. The total fossil flora is composed of 85 pollen types. Concentration, preservation and diversity of the pollen assemblages can be considered very good for a Pleistocene marine succession.

7.2 – Results

The studied interval can be subdivided into short segments characterized by different vegetation states.

Non-arboreal plants are abundant in the lower part of the studied interval (interval A in Fig. 7), corresponding to the late glacial termination of MIS 20. Microthermic forest elements, which increase gradually beginning from the peak $\delta^{18}O$ interglacial, become intermittently dominant at the transition to glacial MIS 18.4 (interval C in Fig. 7). The $\delta^{18}O$ interval corresponding to the full MIS 19 interglacial is predictably dominated by mesothermic broadleaved forest trees (interval B in Fig. 7).

By comparison to the present-day distribution of vegetation in the Central Mediterranean area, the abundance of herbs and steppe plants during the demise of glacial MIS 20 points to very dry climates (Capraro *et al.*, 2005 and references therein; Bertini *et al.*, 2015). Still, one may speculate that during the glacial termination of MIS 20, the sea-level rise forced the fluvial entry-points to retreat landwards. This process may have stopped the conveyance of arboreal pollen from the inner mainland, which mainly occurs via river runoff, in favor of airborne grains of herbs and shrubs that thrived in the surrounding lowlands and littoral areas (Capraro *et al.*, 2005).

The full MIS 19 interglacial is characterized by the extremely high abundances of temperate (mesothermic) forest elements (Fig. 7), such as *Tilia*, *Carpinus* and *Ostrya*, being deciduous *Quercus* the dominant pollen type. Evergreen trees, such as *Quercus ilex*, *Olea* and *Phillyrea* are also well represented. This forest assemblage is overall similar to the vegetation that nowadays prospers in the inner mainland of the Mediterranean regions (Noirfalise *et al*., 1987), suggesting that MIS 19 was characterized by a "modern" vegetation and a climate similar to the present day. However, we observed a significant amount of pollen grains of "Tertiary" elements, such as *Carya* and *Pterocarya*, presently not indigenous in the Mediterranean basin (e.g., Bertini, 2003).

"Exotic" elements (namely *Picea*, *Tsuga* and *Cedrus*) are also common within the "mountain"

(boreal) group, which is generally dominated by *Abies*. This assemblage points to cool/cold climates, with a minimum annual rainfall rate much higher than the present day in the Central Mediterranean area. The "mountain" group becomes relevant only at the demise of MIS 19, i.e. during the onset of the MIS 18 glaciation (interval C in Fig. 7). This interval is characterized by a marked instability in both $\delta^{18}O$ and vegetation, which alternates rapidly between two forested states. Specifically, two short-lived intervals of "light" $\delta^{18}O$ are characterized by the increase in "cold" forest elements (CF2 and CF3 events in Fig. 7), while the intervening "heavy" $\delta^{18}O$ episode corresponds to a transient development of the temperate deciduous forest.

As mentioned above, these oscillations may either reflect the altitudinal migration of vegetation belts in response to climate changes, or the amount and type of pollen transport to the basin via river runoff. Specifically, a rise in rainfall rates would increase the fluvial transport of "mountain" pollen grains to the sedimentation area, and vice-versa, independently from the dynamics of vegetation belts. However, we stress that the concurrent erratic behavior of pollen and $\delta^{18}O$ at the MIS 19-MIS 18 transition is hardly incidental, as confirmed by the occurrence of similar sedimentary and isotopic patterns at the MIS 21-MIS 20 transition (Fig. 2).

8 – Magnetostratigraphy

The magnetostratigraphic documentation of the VdM section represents a critical task, given that the M-B reversal is the main criterion for defining the GSSP of the Ionian Stage (Richmond, 1996; Cita *et al.*, 2006; Head *et al.*, 2008). The investigation is discussed thoroughly in a dedicated paper (Macrì *et al.*, submitted), to which we refer for further details. Here, we provide a brief and essential report on the new paleomagnetic record achieved at VdM, which improved dramatically that reconstructed by Rio *et al.* (1996).

8.1 – Materials and methods

In order to better constrain the position of the M-B reversal, we collected 84 *in situ* oriented samples in the stratigraphic interval between -24.80 m and +6.16 m, focusing our attention on the stratigraphic interval encompassing the "Pitagora ash". Measurements were performed at the paleomagnetic laboratory of the Istituto Nazionale di Geofisica e Vulcanologia in Rome by a 2G DC-Squid cryogenic magnetometer. Characteristic remnant magnetization (ChRM) directions of the sediments were isolated by means of an AF demagnetization in 15 steps up to 70 mT and, for 18 specimens, by a stepwise thermal demagnetization in 9 steps up to 420°C. ChRM directions was obtained from 38 samples, with magnetization components isolated by the principal component analysis of Kirschvink (1980).

8.2 – Results

A complete discussion on the magnetostratigraphic and rock magnetic analyses is available in Macrì *et al.* (submitted). Paleomagnetic data indicate that a stable characteristic remanent magnetization (ChRM) can be easily identified for the fine-grained sediments of the entire sequence after the removal of a viscous component at AF<10-20 mT. A persistent normal polarity is documented in the interval from to +0.14 m to +6.16 m, while between +0.00 and +0.11 m samples show a distinct and stable reverse polarity (Fig. 8). From -0.03 to -0.20 m and from –1.05 to – 1.10 m, ChRM directions were computed by fitting a linear component for both thermal and AF demagnetized samples and indicate two short intervals with a normal polarity. A stable inverse polarity was finally reported from -1.10 m to the bottom of the studied interval (-21.35 m). In the dark muds below the "Pitagora ash", acquisition of a spurious gyromagnetic remnant magnetization (GRM) during the AF demagnetization is observed in some samples, confirming that this part of the section contains variable amount of

iron sulphides, probably greigite (Fe3S4). In these cases, the ChRM directions were computed by fitting a straight line to directions measured between 10-20 and 40-50 mT demagnetization steps. The presence of iron sulphides of primary origin in this part of the stratigraphy is supported by a number of rock magnetic analyses (Macrì *et al.*, submitted).

Our data provide an unequivocal recognition of the paleomagnetic polarity, which pinpoints the M-B reversal to a 3 cm-thick interval (between +0.11 and +0.14 m; midpoint of the transition at +0.125 m) above the base of the "Pitagora ash", in the midst of MIS 19.

9 – Discussion

The data presented in this paper yielded new and essential information on the VdM section, especially in terms of timing and duration of the main events that characterize the Early-Middle Pleistocene transition. It is held that the physical stratigraphic organization of the VdM section reflects in detail the dynamics of regional and global climates, which are validated by several proxies, such as stable oxygen isotopes, calcareous nannofossils, pollen and mollusk faunas.

The collected data point univocally to a continuous and undisturbed stratigraphic record of the MIS 20-MIS 18 interval. Based on these evidences, a robust chronostratigraphic framework has been reconstructed for the M-B reversal, which represents a key information for the definition of the GSSP of the Ionian Stage (Richmond, 1996; Cita *et al.*, 2006; Head *et al.*, 2008). We calculated an age of 786.9 ± 0.055 ka for the mid-point of the M-B polarity transition and, according to the estimated sediment accumulation rates (ca. 27 cm/kyr), the geomagnetic flip was probably very fast, in the order of 100 years or less (Macrì et al, submitted). These estimates are in excellent agreement with those calculated by Sagnotti *et al.* (2014) for the Sulmona lacustrine record (Central Italy), where, based on the radiometric dating of several tephra layers, the M-B reversal yielded an age of 786.1 ±

1.5 ka and was also very fast, with an estimated duration of a few decades (Sagnotti *et al.*, 2016). The age of 786.9 ka for the M-B boundary at VdM is also very close to that calculated for the IODP Site U-1313 core, recovered at mid-latitudes in the North Atlantic, where the magnetic flip has an age of 787 ± 1.8 ka, according to the astronomical tuning of the local $\delta^{18}O$ record (Expedition 306 Scientists, 2006; Ferretti *et al.*, 2015). Notably, the VdM, Sulmona and U-1313 records point to a very similar age of the M-B reversal in spite of the different approaches used to develop each of the age models (visual correlation to a regional tuning target, radiometric ages and astronomical tuning, respectively), which rule out the possibility of methodologic biases. Age and duration of the M-B reversal are very debated and still uncertain, in spite of the excellent data collected globally in the last few decades (see Singer, 2014 and Head and Gibbard, 2015 for a review). It was however demonstrated that the age and duration of the M-B transition may vary substantially, depending on the geographical location of the studied record (Clement, 2004). Therefore, there is no rational basis for deeming as "preferred" or "more reliable" any of the proposed chronologies, provided that their scientific background is robust.

At VdM, the midpoint of the M-B reversal is located ca. 12.5 cm above the base of the "Pitagora ash" (Macrì *et al*., submitted), which provides a prominent marker of the geomagnetic event. However, the usefulness of the "Pitagora ash" as physical reference for defining the GSSP of the Ionian Stage was criticized by some, because it may reflect an episode of abrupt resettling of older volcaniclastic material and, in addition, the "Pitagora ash" was not found outside the San Mauro sub-basin (Capraro *et al*., 2011, 2015).

The sedimentary mechanisms that originated the "Pitagora ash" are not clear. It preserves small-scale sedimentary structures, such as plane-parallel lamination and convolutions (Massari *et al.*, 2007). The absence of a basal massive T_a interval is consistent with a low-density turbidity current (*sensu* Lowe, 1982), which prompted Capraro *et al.* (2015) to describe the "Pitagora ash" as a

"resedimented" layer. However, the presence of sedimentary structures is not sufficient to determine whether it represents a "primary" tephra or a product of resedimentation of older volcaniclastic material (Mezzetti *et al.*, 1991; Manville and Wilson, 2004; Manville *et al*., 2009). Indeed, discriminating between "primary" tephra layers, generated from ash falling and settling, and "secondary" deposits, originated from the resettling of older volcaniclastic material, is generally not possible (Carey & Sigurdsson, 1978; Sparks *et al.*, 1983; Manville & Wilson, 2004).

In an open marine setting, the deposition and preservation of thick layers of fine-grained volcaniclastic materials can hardly be interpreted as the response to pure ash fall and settling (Huang, 1980). In a pure settling regime, ash particles would sink over months to decades, and bioturbation would immediately disperse in the sediment the slowly accumulating volcaniclastics (Manville & Wilson, 2004). Actually, tephra layers are usually characterized by a sharp base, implying a massive and abrupt suppression of the benthic fauna, and a bioturbated top, in response to the subsequent recolonization of the sea floor (Cita and Podenzani, 1980; Marquez, 2000), demonstrating that the sedimentation process was extremely fast.

Anyhow, the possible occurrence of a single event of sediment resettling would not imply a persistent turbiditic regime in the buildup of the local succession. Indeed, macrofossils do not show evidence of preferred orientation, lags or reworking in the whole SM2 unit (Scarponi *et al*., 2014). The "Pitagora ash" is the sole evidence consistent with a sedimentary process other than mud settling in the whole SM2 interval, where the fine fraction originated from fallout (see also Massari *et al.*, 2002 and 2007), as reasonably expected in any sedimentary succession accumulated below the storm wave base (Clifton, 2006).

It is suggested that also in the coeval Montalbano Jonico and Chiba sections, where the sediment accumulation rates are much higher in response to a persistent turbiditic regime (Ciaranfi *et al*., 2010; Kazaoka *et al*., 2015), the deposition of tephra layers was massive and abrupt. Otherwise,

volcaniclastic deposits would be completely dispersed by dilution and/or bioturbation in the embedding sediments (Manville & Wilson, 2004).

Reasonably, preservation of the "Pitagora ash" in the San Mauro sub-basin as a distinctive horizon was only possible because whitish volcaniclastic material was laid within the dark, hypoxic and hardly bioturbated muds of MIS 19 (Fig. 2), where sediment mixing was extremely weak; in open-marine and well-oxygenated settings, such as the neighboring Marcedusa sub-basin, the correlative tephra layer was probably destroyed (Capraro et al., 2011).

The lack of horizontal continuity of the "Pitagora ash" outside the San Mauro sub-basin is not surprising because, since the early work of Steno (1669), it is common knowledge that sedimentary layers do not extend indefinitely, being their limits circumscribed by the shape and size of the basin where, by definition, they were laid. Not by chance, the lateral (horizontal) physical continuity of strata is not contemplated among the guidelines for the definition of a GSSP (Remane *et al.*, 1996). By contrast, an excellent long-distance correlation potential is demanded for the "most relevant marker events" that approximate the boundary (Remane *et al.*, 1996). In defining the GSSP of the Ionian Stage, the "most relevant marker event" – i.e., the main guide criterion – is the M-B boundary (Richmond, 1996; Cita *et al.*, 2006; Head *et al.*, 2008), which can be pinpointed easily in the VdM section (Fig. 8). Therefore, other than being a mere tool for stratigraphic correlation at the basin scale, the "Pitagora ash" can be perfectly employed as a marker bed for assessing the stratigraphic position of the M-B boundary and, consequently, to serve as the physical reference level for defining of the GSSP of the Ionian Stage.

Furthermore, the VdM section represents one of the component segments of the composite stratigraphic succession of the Crotone Basin (Capraro *et al.*, 2011), where the GSSP of the Calabrian Stage was defined (Vrica section; Pasini and Colalongo, 1997; Cita *et al*., 2012). Indeed, the stratigraphic succession exposed in the San Mauro sub-basin and neighboring areas extends well

below the base of the Calabrian and, once framed in the context of the local stratigraphic succession, the VdM section can be physically linked to the Vrica section for defining the Unit Stratotype for the Calabrian Stage.

10 – Conclusions

Data presented and discussed in this paper demonstrate that the VdM section stands out as an excellent candidate to host the GSSP of the Ionian Stage. This assumption is based on the following evidences:

- the VdM section ensures a continuous and very well-documented record of the interval between upper MIS 22 and MIS 18. In particular, the section provides an excellent record of the MIS 19 interglacial, where the GSSP should be placed;
- the VdM section boasts a razor-sharp record of the M-B magnetic reversal, the age of which (ca. 786.9 ka), obtained by tuning to the open-sea $\delta^{18}O$ records, is in full agreement with many records globally (e.g., the Sulmona paleolake; Sagnotti *et al.*, 2014);
- the VdM section fulfills all the requirements of Remane *et al.* (1996) for the definition of the GSSP of the Ionian Stage (good and easily accessible exposure, continuous and expanded open-marine sedimentation, absence of synsedimentary and tectonic disturbances, abundant and diversified fossils, absence of vertical facies changes near the boundary, etc.).

Hence, we propose that the GSSP of the Ionian Stage (base of the Middle Pleistocene Subseries) should be defined at the very base of the "Pitagora ash", i.e. 12.5 cm below the mid-point of the M-B magnetic reversal (Macrì *et al*., submitted). We insist that defining all the GSSPs of the Neogene in a similar geographic and depositional setting (i.e., the Mediterranean basin) would represent a huge

benefit, because correlation among contiguous sedimentary basins is straightforward and can take advantage of a regionally-validated calibration of the main biomagnetostratigraphic proxies.

Acknowledgments

This research was funded by the University of Padova (Progetto di Ateneo 2010 and ex-60% to L. Capraro). We are thankful to C. Betto, N. Preto and C. Agnini for technical assistance.

lunedì 29 agosto 2016

REFERENCES

Backman, J., Shackleton, N.J., 1983. Quantitative biochronology of Pliocene and early Pleistocene calcareous nannoplankton from the Atlantic Indian and Pacific Oceans. Mar. Micropaleontol. 8, 141-170.

Barone, A., Fabbri, A., Rossi, S., Sartori, R., 1982. Geological structure and evolution of the marine area adjacent to the Calabrian Arc. Earth Planet. Sci. Lett. 3, 207-221.

Bensi, M., Rubino, A., Cardin, V., Hainbucher, D., ManceroMosquera, I., 2013. Structure and variability of the abyssal water masses in the Ionian Sea in the period 2003–2010., J. Geophys. Res. 118, 1-13. doi:10.1029/2012JC008178.

Bertini, A., 2003. Early to Middle Pleistocene changes of the Italian flora and vegetation in the light of a chronostratigraphic framework. Il Quaternario, 16, 19-36.

Bertini, A., Toti, F., Marino, M., Ciaranfi, N., 2015. Vegetation and climate across the Early-Middle Pleistocene transition at Montalbano Jonico, southern Italy. Quat. Int. 383, 74-88.

Béthoux, J., Morin, P., Madec, C., Gentill, B., 1992. Phosphorus and nitrogen behaviour in the Mediterranean Sea. Limnol. Oceanogr. 39, 1641-1654.

Borzelli, G.L.E., Gačić, M., Cardin, V., Civitarese, G., 2009. Eastern Mediterranean Transient and reversal of the Ionian Sea circulation. Geophys. Res. Lett. 36, L15108. doi:10.1029/2009GL039261.

Capraro, L., Asioli, A., Backman, J., Bertoldi, R., Channell, J.E.T., Massari, F., Rio, D., 2005. Climatic patterns revealed by pollen and oxygen isotope records across the Brunhes-Matuyama boundary in the central Mediterranean (Southern Italy). In: Head, M.J., Gibbard, P.L. (Eds.), Geol. Soc. Lond. Spec. Publ. 247, Geological Society, Bath, UK, pp. 159-182.

Capraro, L., Consolaro, C., Fornaciari, E., Massari, F., Rio, D., 2006. Chronology of the Middle-Upper Pliocene succession in the Strongoli area: constraints on the geological evolution of the Crotone Basin (Southern Italy). In: Moratti, G., Chalouan, A. (Eds.), Tectonics of the Western Mediterranean and North Africa. Geol. Soc. Lond. Spec. Publ. 262 Geological Society, Bath, UK, pp. 323-333.

Capraro, L., Macrì, P., Scarponi, D., Rio, D., 2015. The lower to Middle Pleistocene Valle di Manche section (Calabria, Southern Italy): state of the art and current advances. Quat. Int. 383, 36-46.

Capraro, L., Massari, F., Rio, D., Fornaciari, E., Backman, J., Channell, J.E.T., Macrì, P., Prosser, G., Speranza, F., 2011. Chronology of the Lower-Middle Pleistocene succession of the south-western part of the Crotone Basin (Calabria, Southern Italy). Quat. Sci. Rev. 30, 1185-1200.

Carey, S.N., Sigurdsson, H., 1978. Deep-sea evidence for distribution of tephra from the mixed magma eruption of the Soufrière on St. Vincent, 1902: ash turbidites and air fall. Geology 6, 271-274.

Castradori, D., 1993. Calcareous nannofossil biostratigraphy and biochronology in eastern Mediterranean deep-sea cores. Riv. Ital. Paleontol. S. 99, 107-126.

Ciaranfi, N., Lirer, F., Lirer, L., Lourens, L.J., Maiorano, P., Marino, M., Petrosino, P., Sprovieri, M., Stefanelli, S., Brilli, M., Girone, A., Joannin, S., Pelosi, N., Vallefuoco, M., 2010. Integrated stratigraphy and astronomical tuning of lower-middle Pleistocene Montalbano Jonico section (southern Italy). Quat. Int. 219, 109-120.

Cita, M.B., Capraro, L., Ciaranfi, N., Di Stefano, E., Marino, M., Rio, D., Sprovieri, R., Vai, G.B., 2006. Calabrian and Ionian: A proposal for the definition of Mediterranean stages for the Lower and Middle Pleistocene. Episodes 29, 107-114.

Cita, M.B., Gibbard, P.L., Head, M.J., 2012. The ICS Subcommission on Quaternary Stratigraphy, 2012. Formal ratification of the GSSP for the base of the Calabrian Stage GSSP (Pleistocene Series,

Quaternary System). Episodes 35, 388-397.

Cita, M.B., Podenzani, M., 1980. Destructive effects of oxygen starvation and ash falls on benthic life: a pilot study. Quaternary Res. 13, 230-241.

Clement, B., 2004. Dependence of the duration of geomagnetic polarity reversal on site latitude. Nature, 428, 637–640.

Clifton, H.E., 2006. A re-examination of facies models for clastic shorefaces. Facies Models Revisited. In: Posamentier, H.W., Walker, R.G. (Eds.), Special Publication No. 84. SEPM (Society for Sedimentary Geology), Tulsa, USA, pp. 293-337.

Coplen, T.B., 1988. Normalization of oxygen and hydrogen isotope data. Chem. Geol. (Isotope Geosci. Sect.) 72, 293-297.

Coplen, T.B., 1994. Reporting of stable hydrogen, carbon, and oxygen isotopic abundances. Pure Appl. Chem. 66, 273-276.

D'Alessandro, A., La Perna, R., Ciaranfi, N., 2003. Response of macrobenthos to changes in paleoenvironments in the Lower-middle Pleistocene (Lucania Basin, Southern Italy). Il Quaternario 16, 167-182.

Elderfield, H., Ferretti, P., Greaves, M., Crowhurst, S.J., McCave, I.N., Hodell, D., Piotrowski, A., 2012. Evolution of ocean temperature and ice volume through the Mid Pleistocene Climate Transition. Science 337, 704-709. doi:10.1126/science.1221294.

Expedition 306 Scientists, 2006. Site U1313. In: Channell, J.E.T., Kanamatsu, T., Sato, T., Stein, R., Alvarez Zarikian, C.A., Malone, M.J., the Expedition 303/306 Scientists, Proc. IODP, 306, Integrated Ocean Drilling Program Management International, Inc., College Station TX. doi:10.2204/iodp.proc.303306.112.2006.

Ferretti, P., Crowhurst, S.J., Naafs, B.D.A., Barbante, C., 2015. The Marine Isotope Stage 19 in the mid-latitude North Atlantic Ocean: astronomical signature and intra-interglacial variability.

Quat. Sci. Rev., 108, 95-110. doi:10.1016/j.quascirev.2014.10.024

Flores, J.A., Gersonde, R., Sierro, F.J., 1999. Pleistocene fluctuations in the Agulhas current retroflection based on the calcareous plankton record. Mar. Micropaleontol. 37, 1-22.

Frew, R.D., Dennis, P.F., Heywood, K.J., Meredith M.P., Boswell, S.M., 2000. The oxygen isotope composition of water masses in the northern North Atlantic. Deep Sea Res.47, 2265-2286.

Gačić, M., Civitarese, G., Eusebi Borzelli, G. L., Kovačević, V., Poulain, P.-M., Theocharis, A., Menna, M., Catucci, A., Zarokanellos, N., 2011. On the relationship between the decadal oscillations of the northern Ionian Sea and the salinity distributions in the eastern Mediterranean. J. Geophys. Res. 116, C12002. doi:10.1029/2011JC007280

Head, M.J., Gibbard, P.L., 2015. Early-Middle Pleistocene transitions: linking terrestrial and marine realms. Quat. Int. 389, 7-46.

Head, M.J., Pillans, B., Farquhar, S., 2008. The Early-Middle Pleistocene Transition: characterization and proposed guide for the defining boundary. Episodes 31, 255-259.

Hemleben, C., Spindler, M., Anderson, O.R., 1989. Modern Planktonic Foraminifera. Springer-Verlag, New York, Berlin, Heidelberg, London, Paris, Tokyo.

Huang, T.C., 1980. A volcanic sedimentation model: implications of processes and responses of deep-sea ashes. Mar. Geol. 38, 103-122.

Kazaoka, O., Suganuma, Y., Okada, M., Kameo, K., Head, M.J., Yoshida, T., Sugaya, M., Kameyama, S., Ogitsu, I., Nirei, H., Aida, N., Kumai, H., 2015. Stratigraphy of the Kazusa Group, Boso Peninsula: An expanded and highly-resolved marine sedimentary record from the Lower and Middle Pleistocene of central Japan. Quat. Int. 383, 116-135.

Kirschvink, J.L., 1980. The least-squares line and plane and the analysis of palaeomagnetic data, Geophys. J. R. Astr. Soc. 62, 699-718.

Lascaratos, A., Williams, R. G., Tragou, E., 1993. A mixed-layer study of the formation of Levantine

Intermediate Water. J. Geophys. Res., 98, 14739-14749.

Lisiecki, L.E., Raymo, M.E., 2005. A Plio-Pleistocene stack of 57 globally distributed benthic $\delta^{18}O$ records. Paleoceanography 20, PA1003. doi:10.1029/2004PA001071

Lourens, L.J., 2004. Revised tuning of Ocean Drilling Program Site 964 and KC01B (Mediterranean) and implications for the $\delta^{18}O$, tephra, calcareous nannofossil, and geomagnetic reversal chronologies of the past 1.1 Myr. Paleoceanography 19, PA3010. doi:10.1029/2003PA000997

Lowe, D.R., 1982. Sediment gravity flows: II Depositional models with special reference to the deposits of high density turbidity currents. J. Sediment. Res. 52, 279-297.

Macrì, P., Speranza, F., Capraro, L., 2014. Magnetic fabric of Plio-Pleistocene sediments from the Crotone fore-arc basin: insights on the recent tectonic evolution of the Calabrian Arc (Italy). J. Geodyn. 81, 67-79.

Maiorano, P., Marino, M., 2004. Calcareous nannofossil bioevents and environmental control on temporal and spatial patterns at the Early-Middle Pleistocene. Mar. Micropaleontol. 53, 405-422.

Malanotte-Rizzoli, P., Bergamasco, A., 1991. The general circulation of the Eastern Mediterranean, Part II: the wind and thermally driven circulation in the baroclinic ocean. Dyn. Atmos. Oceans 15, 355-421

Malanotte-Rizzoli, P., Hecht, A., 1988. Large scale properties of the Eastern Mediterranean: a review. Oceanologica Acta, 11, 323-335

Malanotte-Rizzoli, P., Artale, V., Borzelli-Eusebi, G.L., Brenner, S., Crise, A., Gačić, M., Kress, N., Marullo, S., Ribera d'Alcalà, M., Sofianos, S., Tanhua, T., Theocharis, A., Alvarez, M., Ashkenazy, Y., Bergamasco, A., Cardin, V., Carniel, S., Civitarese, G., D'Ortenzio, F., Font, J., Garcia-Ladona, E., Garcia-Lafuente, J.M., Gogou, A., Gregoire, M., Hainbucher, D., Kontoyannis, H., Kovacevic, V., Kraskapoulou, E., Kroskos, G., Incarbona, A., Mazzocchi, M.G., Orlic, M., Ozsoy, E., Pascual,

A., Poulain, P.M., Roether, W., Rubino, A., Schroeder, K., Siokou-Frangou, J., Souvermezoglou, E., Sprovieri, M., Tintoré, J., Triantafyllou, G., 2014. Physical forcing and physical/biochemical variability of the Mediterranean Sea: a review of unresolved issues and directions for future research. Ocean Sci. 10, 281-322.

Malanotte-Rizzoli, P., Manca, B.B., Ribera d'Acala, M., Theocharis, A., Bergamasco, A., Bregant, D., Budillon, G., Civitarese, G., Georgopoulos, D., Michelato, A., Sansone, E., Scarazzato, P., Souverrmezoglou, E., 1997. A synthesis of the Ionian hydrography, circulation and water mass pathways during POEM—Phase I. Progress in Oceanography, 39, 153-204.

Malanotte-Rizzoli, P., Manca, B.B., Ribera d'Alcalà, M., Theocharis, A., Brenner, A., Budillon, G., Ozsoy, E., 1999. The Eastern Mediterranean in the 80s and in the 90s: The big transition in the intermediate and deep circulations. Dyn. Atmos. Oceans 29, 365-395.

Marquez, E.J., 2000. The 1991 Mount Pinatubo eruption and Eastern South China Sea foraminifera: occurrence, composition and recovery. Island Arc 9, 527-541.

Massari, F., Capraro, L., Rio, D., 2007. Climatic modulation of timing of systems-tract development with respect to sea-level changes (middle Pleistocene of Crotone, Calabria, Southern Italy). J. Sediment. Res. 77, 461-468.

Massari, F., Rio, D., Sgavetti, M., Prosser, G., D'Alessandro, A., Asioli, A., Capraro, L., Fornaciari, E., Tateo, F., 2002. Interplay between tectonics and glacio-eustasy: Pleistocene succession of the Crotone Basin, Calabria (Southern Italy). Geol. Soc. Am. Bull. 114, 1183-1209.

Massari, F., Sgavetti, M., Rio, D., D'Alessandro, A., Prosser, G., 1999. Sedimentary record of falling stages of Pleistocene glacio-eustatic cycles in shelf setting (Crotone Basin, south Italy). Sediment. Geol. 127, 85-110.

Massari, F., Prosser, G., Capraro, L., Fornaciari, E., Consolaro, C., 2010. A revision of the stratigraphy and geology of the south-western part of the Crotone basin (Southern Italy). Ital. J. Geosci. 129, 353-384.

Manville, V., Wilson, C.J.N., 2004. Vertical density currents: a review of their potential role in the deposition and interpretation of deep-sea ash beds. J. Geol. Soc. London 161, 947-958.

Manville, V., Németh, K., Kano, K., 2009. Source to sink: A review of three decades of progress in the understanding of volcaniclastic processes, deposits, and hazards. Sediment. Geol. 220, 136-161.

Melinte, M.C., 2005. Calcareous nannoplankton, a tool to assign environmental changes. Geo-Eco-Marina 7-8, 136-143.

Mezzetti, R., Morandi, N., Tateo, F., Dondi, M., 1991. Il contributo vulcanoderivato in successioni pelitiche oligomioceniche dell'Appennino settentrionale. G. Geol. 53, 167-185.

Noirfalise, A., Dahl, E., Ozenda, P., Quezél, P., Bohn, W., Trautmann, W., Wagner, H., Rivas-Martinez, S., Rameau, J.C., Mavrommatis, G., Einarsson, E., Gentile, S., Tomaselli, R., Kalkhoven, J.T.R., Malato-Beliz, J., Newbold, C., Pahlsson, L., Baum, P., Ribaut, J.P. & Cornaert, M.H., 1987. Carte de la vegetation naturelle des Etats membres des Communautés européennes et du Conseil de l'Europe. Office des publications des Communautés européennes, Luxembourg.

Pasini, G., Colalongo, M.L., 1997. The Pliocene-Pleistocene boundary stratotype at Vrica, Italy. In: Van Couvering, J. (ed.), The Pleistocene boundary and the beginning of the Quaternary. Cambridge University Press, Cambridge, U.K., pp. 1545.

Pierre, C., 1999. The oxygen and carbon isotope distribution in the Mediterranean water masses. Mar. Geol. 153, 41-55.

Pillans, B., Gibbard, P.L., 2012. Chapter 30: The Quaternary Period. In: Gradstein, F.M., Ogg, J., Schmitz, M., Ogg, G. (Eds.), The Geologic Time Scale 2012. Elsevier, Amsterdam, 980-1010.

Pujol, C., Vergnaud-Grazzini, C., 1995. Distribution patterns of live planktonic foraminifera as related to regional hydrography and productive systems of the Mediterranean Sea. Mar. Micropaleontol. 25, 187-217.

Raffi, I., Backman, J., Fornaciari, E., Pälike, H., Rio, D., Lourens, L., Hilgen, F., 2006. A review of calcareous nannofossil astrobiochronology encompassing the past 25 million years. Quat. Sci. Rev. 25, 3113-3137.

Remane, J., Bassett, M.G., Cowie, J.W., Gohrbandt, K.H., Lane, H.R., Michelsen, O., Wang, N., 1996. Revised guidelines for the establishment of global chronostratigraphic standards by the International Commission on Stratigraphy (ICS). Episodes 19, 77-81.

Richmond, G.M., 1996. The INQUA-approved provisional Lower-Middle Pleistocene boundary. In: Turner, C. (Ed.), The Early-Middle Pleistocene in Europe. Balkema, Rotterdam, pp. 319-326.

Rio, D., 1982. The fossil distribution of Coccolithophore Genus *Gephyrocapsa* KAMPTNER and related Plio-Pleistocene chronostratigraphic problems. In: Prell, W.L., Gardner, J.V., *et al.* (Eds.), Proceedings of the Deep Sea Drilling Project, Initial Reports, vol. 68. Deep Sea Drilling Project, Washington, DC, US Government Printing Office, pp. 325-343.

Rio, D., Channell, J.E.T., Massari, F., Poli, M.S., Sgavetti, M., D'Alessandro, A., Prosser, G., 1996. Reading Pleistocene eustasy in a tectonically active siliciclastic shelf setting (Crotone peninsula, Southern Italy). Geology 24, 743-746.

Rio, D., Sprovieri, R., Di Stefano, E., 1998. The Gelasian Stage (Upper Pliocene): a new unit for the global standard chronostratigraphic scale. Episodes 21, 82-87.

Robinson, A.R., Golnaraghi, M., Leslie, W.G., Artegiani, A., Hecht, A., Lazzoni, E., Michelato, A., Sansone, E.A., Theocharis, A., Unluata, U., 1991. Structure and variability of the Eastern Mediterranean general circulation. Dyn. Atm. Oceans 15, 215-240

Roda, C., 1964. Distribuzione e facies dei sedimenti Neogenici del Bacino Crotonese. Geol. Rom. 3, 319-366.

Rossi, S., Sartori, R., 1981. A seismic reflection study of the external Calabrian Arc in the northern Ionian Sea (eastern Mediterranean). Mar. Geophys. Res. 4, 403-426.

Sagnotti, L., Scardia, G., Giaccio, B., Liddicoat, J.C., Nomade, S., Renne, P.R., Sprain, C.J., 2014. Extremely rapid directional change during Matuyama-Brunhes geomagnetic polarity reversal. Geophys. J. Int. 199, 1110-1124.

Sagnotti, L., Renne, P.R., Giaccio, B., Scardia, G., Liddicoat, J.C., Sprain, C.J., Nomade, S., 2016 How fast was the Matuyama-Brunhes geomagnetic reversal? A new subcentennial record from the Sulmona Basin, central Italy. Geophys. J. Int. 204, 798-812.

Scarponi, D., Huntley, J.W., Capraro, L., Raffi, S., 2014. Stratigraphic paleoecology of the S. Mauro Marchesato Section (Crotone Basin, Italy): a candidate GSSP of the Middle Pleistocene. Palaeogeogr. Palaeoclimatol. Palaeoecol. 402, pp. 30-43.

Shackleton, N.J., 1967. Oxygen isotope analyses and Pleistocene temperatures re-assessed. Nature 215, 15-17.

Shackleton, N.J., 1974. Attainment of isotopic equilibrium between ocean water and the isotopic equilibrium of the benthonic foraminifera genus *Uvigerina*: isotopic changes in the ocean during the last glacial. Les methods quantitatives d'etude des variations du climat au cours du Pleistocene, Gif-sur-Yvette. Colloque international du CNRS, 219, 203-210.

Singer, B.S., 2014. A Quaternary geomagnetic instability time scale, Quat. Geochron., 21, 29–52.

Sparks, R.S.J., Brazier, S., Huang, T.C., Muerdter, D. 1983. Sedimentology of the Minoan deep-sea tephra layer in the Aegean and Eastern Mediterranean. Mar. Geol. 54, 131-167.

Sprovieri, R., Di Stefano, E., Howell, M., Sakamoto, T., Di Stefano, A., Marino, M., 1998. Integrated calcareous plankton biostratigraphy and cyclostratigraphy at Site 964. In: Robertson, A.H.F., Emeis, K.C., Richter, C., Camerlenghi, A. (Eds.), Proceedings Ocean Drilling Program, Scientific Results, vol. 160. Ocean Drilling Program, College Station, TX, pp. 155-165.

Sprovieri, R., Di Stefano, E., Incarbona, A., Gargano, M.E., 2003. A high-resolution record of the last deglaciation in the Sicily channel based on foraminifera and calcareous nannofossil quantitative distribution. Palaeogeogr. Palaeoclimatol. Palaeoecol. 202, 119-142.

Stefanelli, S., 2003. Benthic foraminiferal assemblages as tools for paleoenvironmental reconstruction of the early-middle Pleistocene Montalbano Jonico composite section. B. Soc. Paleontol. Ital. 42, 281-299.

Steno, N., 1669. De solido intra solidum naturaliter contento dissertationis prodromus. Stella, Florence.

Suganuma, Y., Okada, M., Horie, K., Kaiden, H., Takehara, M., Senda, R., Kimura, J., Kawamura, K., Haneda, Y., Kazaoka, O., Head, M.J., 2015. Age of Matuyama–Brunhes boundary constrained by U-Pb zircon dating of a widespread tephra. Geology, 43, 491–494. doi:10.1130/G36625.1

Tanhua, T., Hainbucher, D., Schroder, K., Cardin, V., Alvarez, M., Civitarese, G., 2013. The Mediterranean Sea system: a review and an introduction to the special issue. Ocean Sci. Discuss. 10, 581- 617. doi:10.5194/osd-10-581-2013.

Thierstein, H.R., Geitzenauer, K., Molfino, B., Shackleton, N.J., 1977. Global synchroneity of late Pleistocene coccolith datum levels; validation by oxygen isotopes. Geology 5, 400-404.

Van Dijk, J.P., Okkes, M., 1991. Neogene tectonostratigraphy and kinematics of Calabrian basins; implications for the geodynamics of the Central Mediterranean. Tectonophysics 196, 23-60.

Vergnaud-Grazzini, C., Devaux, M., Znaidi, J., 1986. Stable isotope "anomalies" in the Mediterranean Pleistocene records. Mar. Micropaleontol. 10, 35-69.

Villa, G., Palandri, S., Wise, S.W., 2005. Quaternary calcareous nannofossils from Periantarctic basins: Paleoecological and paleoclimatic implications. Mar. Micropaleontol. 56, 103-121.

Wells, P., Okada, H., 1996. Holocene and Pleistocene glacial palaeoceanography off southeastern Australia, based on foraminifers and nannofossils in Vema cored hole V18-222. Aust. J. Earth Sci. 43, 509-523.

Wells, P., Okada, H., 1997. Response of nannoplankton to major changes in sea-surface temperature and movements of hydrological fronts over Site DSDP 594 (South Chatham Rise, southeastern New Zealand), during the last 130 kyr. Mar. Micropaleontol. 32, 341-363.

Wüst, G., 1961. On the vertical circulation of the Mediterranean Sea. J. Geophys. Res. 66, 3261-3271.

lunedì 29 agosto 2016

TABLE CAPTIONS

Table 1 – Description of the facies recognized in the Valle di Manche section and employed in Fig. 2.

Table 2 – Stratigraphic and chronostratigraphic position of the control points employed for reconstructing the age model for Valle di Manche section and their age. The average sediment accumulation rates calculated between contiguous tie points are also reported.

FIGURE CAPTIONS

Figure 1 – a) location of the Crotone Basin in Southern Italy; b) simplified geologic map of the Crotone Basin and location of the San Mauro area; c) location of the Valle di Manche (VdM) section, south of the San Mauro Marchesato village; d) view of the Valle di Manche outcrop, exposed below the cemetery of San Mauro Marchesato. The SM1, SM2 and SM3 units are indicated. The dashed line indicates the position of the "Pitagora ash". The thin vertical line marks the sampling profile.

Figure 2 – Physical stratigraphy and $\delta^{18}O$ stratigraphy for *Uvigerina peregrina* of the VdM section. See table 1 for facies description.

Figure 3 – The upper thermohaline circulation and water mass pathways in the central Mediterranean (modified from Malanotte-Rizzoli *et al*., 2014). Dashed and solid lines mark water mass pathways and permanent dynamic features, respectively. AIS: Atlantic-Ionian Stream. MAW: Modified Atlantic Waters. IA: Ionian Anticyclones. MIJ: Mid-Ionian Jet. C: position of the Crotone Basin. K: position of Core KC01b (Castradori, 1993).

Figure 4 – Age model for the Valle di Manche section (thin black line) derived by comparison to the Mediterranean Stack of Lourens (2004), indicated by the thick grey line. The utilized control points are designated by open diamonds.

Figure 5 – Comparison between the $\delta^{18}O$ record of *U. peregrina* and the local paleodepths calculated by Scarponi *et al.* (2014). MED: Maximum Eustatic Depth. LMD: Local Maximum Depth. The dashed segment in the paleodepth curve correlates to the putative eustatic low of MIS 20, where the mollusk fauna is sparse and statistically insignificant.

Figure 6 – Distribution of diagnostic nannofossil species. a) total abundance of gephyrocapsids (in terms of number of specimens per mm^2) compared to the local $\delta^{18}O$ record of *U. peregrina*. b) abundance of *G. oceanica* (specimens/mm^2). c,d) percentile abundances of *G.* sp.3/*omega* and *G. caribbeanica* with respect to the total gephyrocapsids assemblage. e) qualitative estimates of the reworking within the nannofossil assemblage (thick line), showing a remarkable anticovariant trend with respect to the local $\delta^{18}O$ record of *U. peregrina* (thin line). Gray bands indicate the position of the local maximum depth (LMD) intervals of MIS 21 and MIS 19. td2 beginning: base of the temporary disappearance of *G.* sp.3/*omega*.

Figure 7 – Pollen record across MIS 19 from the Valle di Manche section. The $\delta^{18}O$ record of *U. peregrina* (left) is compared to ecologically significant vegetation groups. Far right: subdivision of the pollen record into ecozones with climatic significance. CF1-3: short-lived events of increasing boreal (“cold”) forest, suggesting cool/cold and humid climates. NA1-

2: intervals with prominent abundances of non-arboreal plants, indicative of arid conditions. LMD: Local Maximum Depth.

Figure 8 – Paleomagnetic results from the Valle di Manche section. a) tilt-corrected ChRM inclinations and correlative magnetic polarity zones paralleled to the $\delta^{18}O$ record of *U. peregrina* (thick gray line). Black solid dots: normal polarity; white dots: reverse polarity. C1r: Matuyama Chron; C1n: Brunhes Chron. b) detail in the interval straddling the M-B boundary. Thicknesses of the "Pitagora ash" are reported to scale.

Table 1

Facies	Description
A	Dark, massive muds, mainly silty clays, that contain large dispersed burrows and sulphide nodules. The benthic foraminifer fauna is scanty and oligospecific, being dominated by *Uvigerina peregrina* , *Brizalina* spp. and *Bulimina marginata* . This facies is indicative of fine-grained substrates in an outer shelf setting, with high fluxes of organic matter. Oxygenation at the seafloor was poor especially in the lower half of the unit, where the mollusk fauna is very scarce (Scarponi *et al* ., 2014) and mainly represented by a juvenile assemblage dominated by *Corbula gibba* , indicative of hypoxic conditions (Ceregato *et al* ., 2007) and/or high sediment accumulation rates (Scarponi and Angeletti, 2008).
B	Detritic firmgrounds mantled by biogenic concentrations of the gregarious deep-sea ostreid *Neopycnodonte cochlear* . Shells are embedded in a matrix of mud (mainly clayey silts), pointing to conditions of minimum sediment accumulation rates (starvation) in an outer shelf-upper slope setting (Scarponi *et al* ., 2014).
C1	Massive, unconsolidated muddy silts very rich in bryozoans and unsorted skeletal material, indicative of intense in situ macrofaunal fragmentation. The benthic foraminiferal assemblage is dominated by *Cassidulina laevigata* ; epiphytic forms increase in abundance upwards, suggesting a gradual transition from an outer to a mid-shelf setting.
C2	Couplets of alternating light, skeletal-rich layers of overcompacted coarse silts and dark, poorly fossiliferous layers of soft muds. The thickness of individual strata is ca. 20 cm. The base of this unit is marked by a distinctive, ~10 cm-thick blackish layer rich in *Chondrites* (Ch in Fig. 2) that points to short-lived episode of reduced oxygenation at the bottom.
C3	Massive silts with dispersed autochthonous skeletal material (mainly mollusks) and sparse vegetal remains that increase in abundance upwards. The benthic foraminiferal fauna is dominated by *Cassidulina* spp. and *Elphidium* spp. associated with *Bulimina marginata* and *Bolivina catanensis* . The occurrence of shells in life position suggests a low-energy environment with frequent mud blanketing in a mid-shelf environment, grading upwards to a prodelta setting.
D	Massive, fine to coarse silts alternating with sharp-based, planar-laminated, generally thin-bedded tabular to lenticular layers of fine micaceous sands (sand/mud ratio between 1/10 and 1/5). Stringers of vegetal debris and plant macrorests are extremely abundant. Restricted to the upper part of the SM1 unit, sparse shells of *Arctica islandica* are also present. Benthic foraminiferal assemblages are similar to those of facies C3. The depositional setting is a distal to intermediate delta-front, where a background sedimentation sustained by mud settling was punctuated by the emplacement of thin sandy layers in response to high-energy events, such as river floods and/or storm-induced flows.
E	An individual layer, ca. 40 cm-thick, of medium to coarse silts and fine sands with a loosely packed concentration of the gastropod *Turritella tricarinata* , locally associated with sparse pectinids. Benthic foraminiferal assemblages are similar to those of facies C3. The inferred environment is a prodelta (mid-shelf) setting subjected to high sedimentation rates, possibly under the influence of riverine waters (Huntley and Scarponi, 2012).

Table 1

Table 2

Level (m)	Age (ka)	Description	Average sediment accumulation rates (cm/kyr)
13.31	740	MIS 18	
			29
8.06	758	MIS 18	
			31
2.81	775	Glacial inception of MIS 20	
			20
1.20	783	Peak MIS 19	
			27
-1.75	794	Midpoint of MIS 20-MIS 19 transition	
			94
-10.25	803	MIS 20	
			42
-15.50	815	MIS 20	
			5
-16.50	836	MIS 21.2	
			15
-18.25	848	MIS 21.3	
			10
-19.50	861	MIS 21.5	
			58
-23.00	866	Midpoint of MIS 22-MIS 21 transition	

Table 2

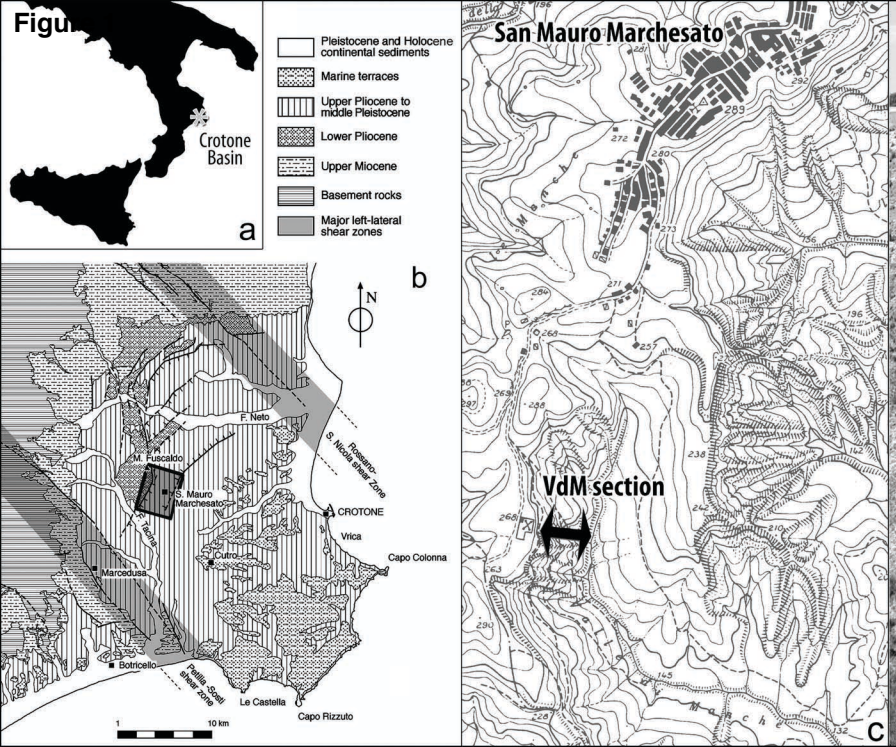
Figu
Pleistocene and Holocene continental sediments
Marine terraces
Upper Pliocene to middle Pleistocene
Lower Pliocene
Upper Miocene
Basement rocks
Major left-lateral shear zones
Crotone Basin
a
b
N
F. Neto
M. Fuscaldo
S. Mauro Marchesato
Rossano-S. Nicola shear Zone
CROTONE
Vrica
Capo Colonna
Cutro
Marcedusa
Botricello
Petilia Soder shear zone
Le Castella
Capo Rizzuto
1
10 km
San Mauro Marchesato
VdM section
c
d
SM3
SM2
SM1

Figure 2

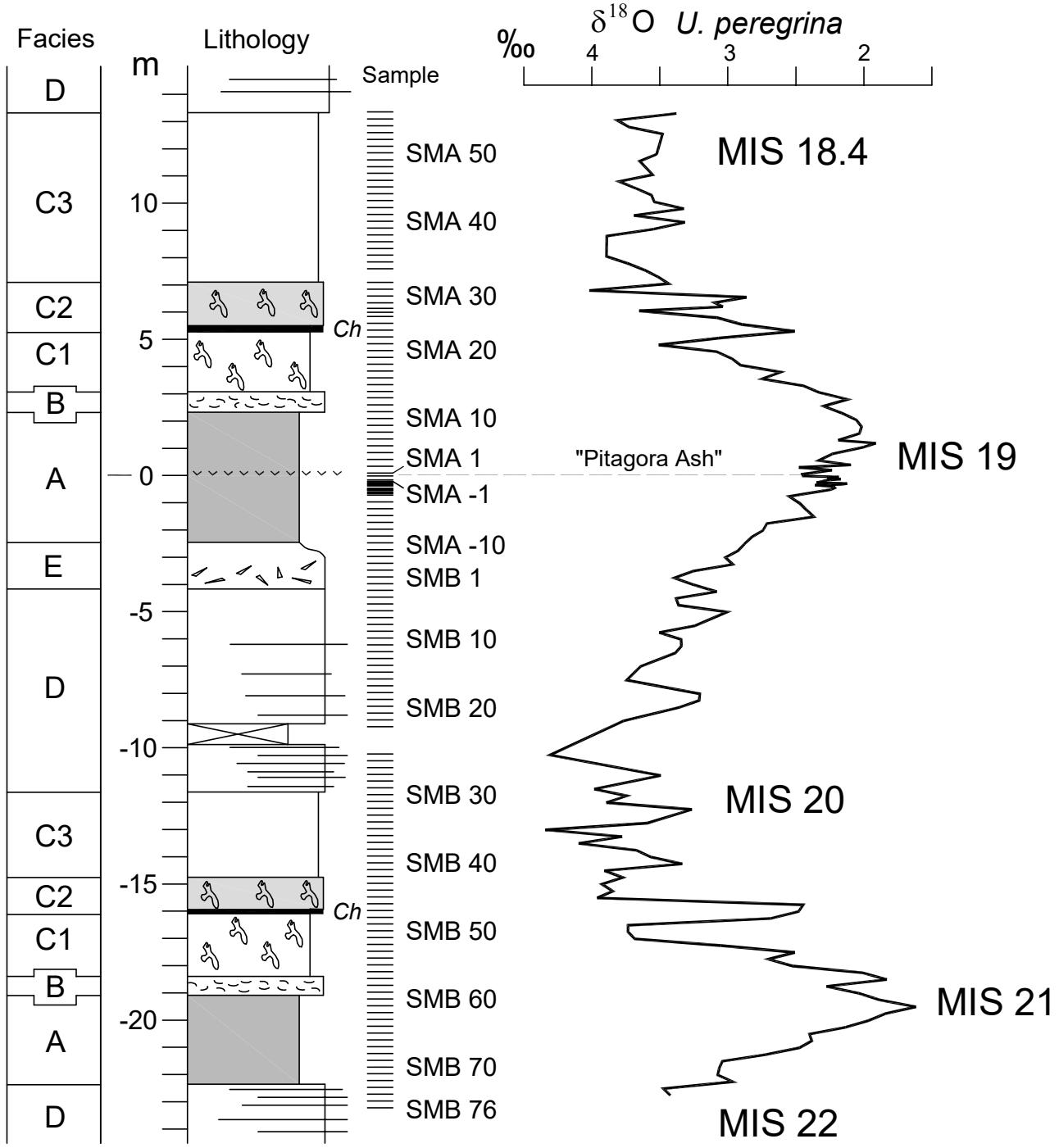
Facies
Lithology
m
Sample
δ18O U. peregrina
‰
4
3
2
D
C3
C2
C1
B
A
E
D
C3
C2
C1
B
A
D
10
5
0
-5
-10
-15
-20
Ch
Ch
SMA 50
SMA 40
SMA 30
SMA 20
SMA 10
SMA 1
SMA -1
SMA -10
SMB 1
SMB 10
SMB 20
SMB 30
SMB 40
SMB 50
SMB 60
SMB 70
SMB 76
"Pitagora Ash"
MIS 18.4
MIS 19
MIS 20
MIS 21
MIS 22

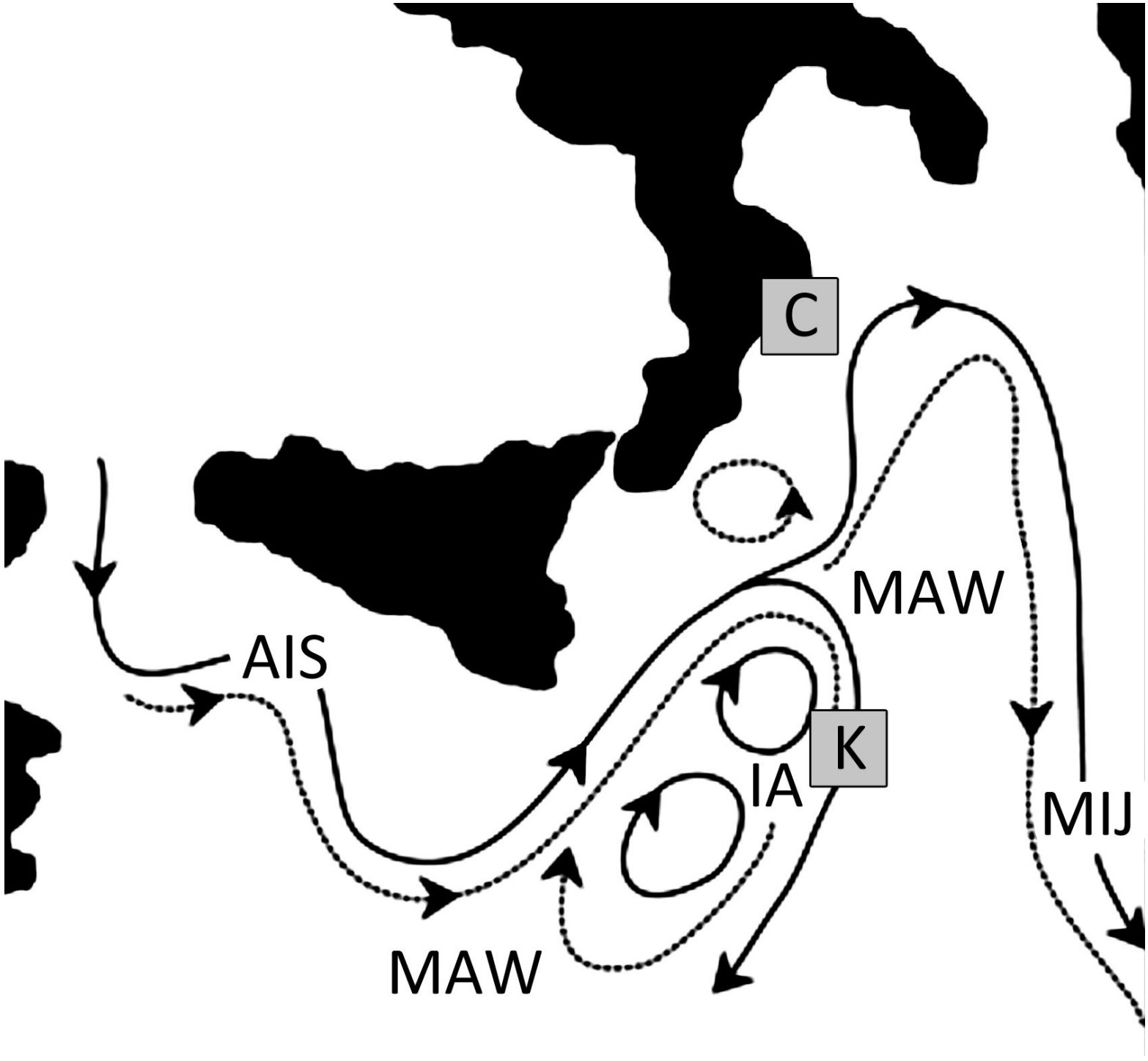
C
MAW
AIS
K
IA
MIJ
MAW

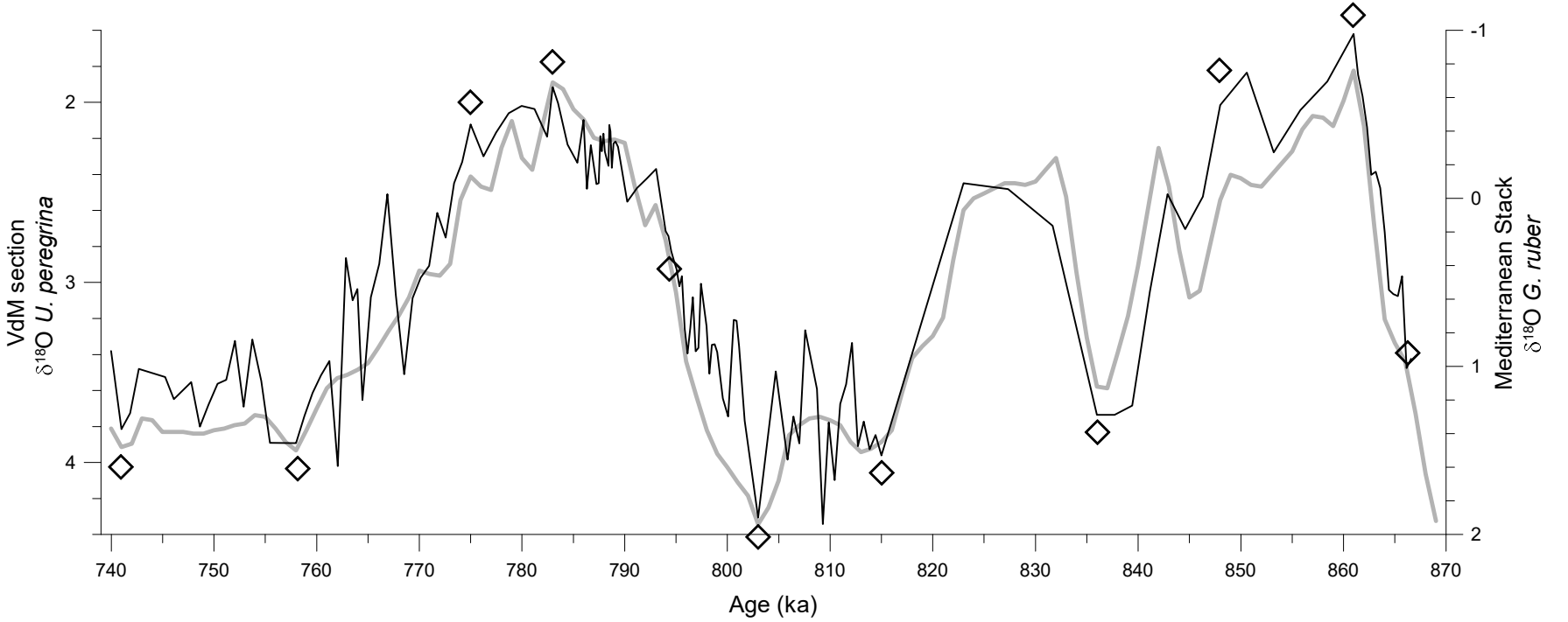
VdM section
δ18O U. peregrina
Mediterranean Stack
δ18O G. ruber
Age (ka)
2
3
4
-1
0
1
2
740
750
760
770
780
790
800
810
820
830
840
850
860
870

Figure 5

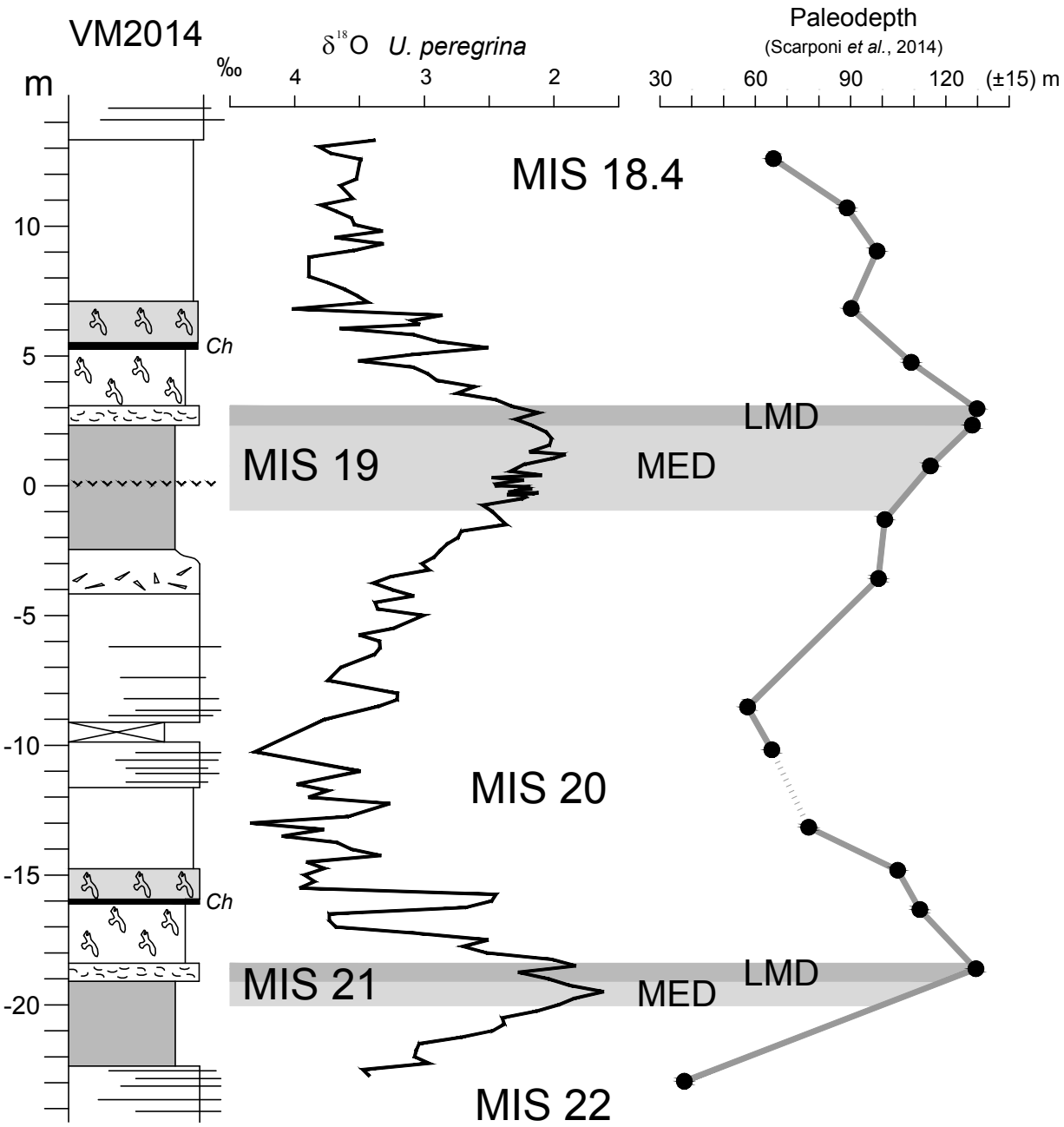
VM2014
m
δ18O U. peregrina
‰
4
3
2
Paleodepth
(Scarponi et al., 2014)
30
60
90
120
(±15) m
10
5
0
-5
-10
-15
-20
Ch
Ch
MIS 18.4
LMD
MIS 19
MED
MIS 20
MIS 21
MED
LMD
MIS 22

Figure 6

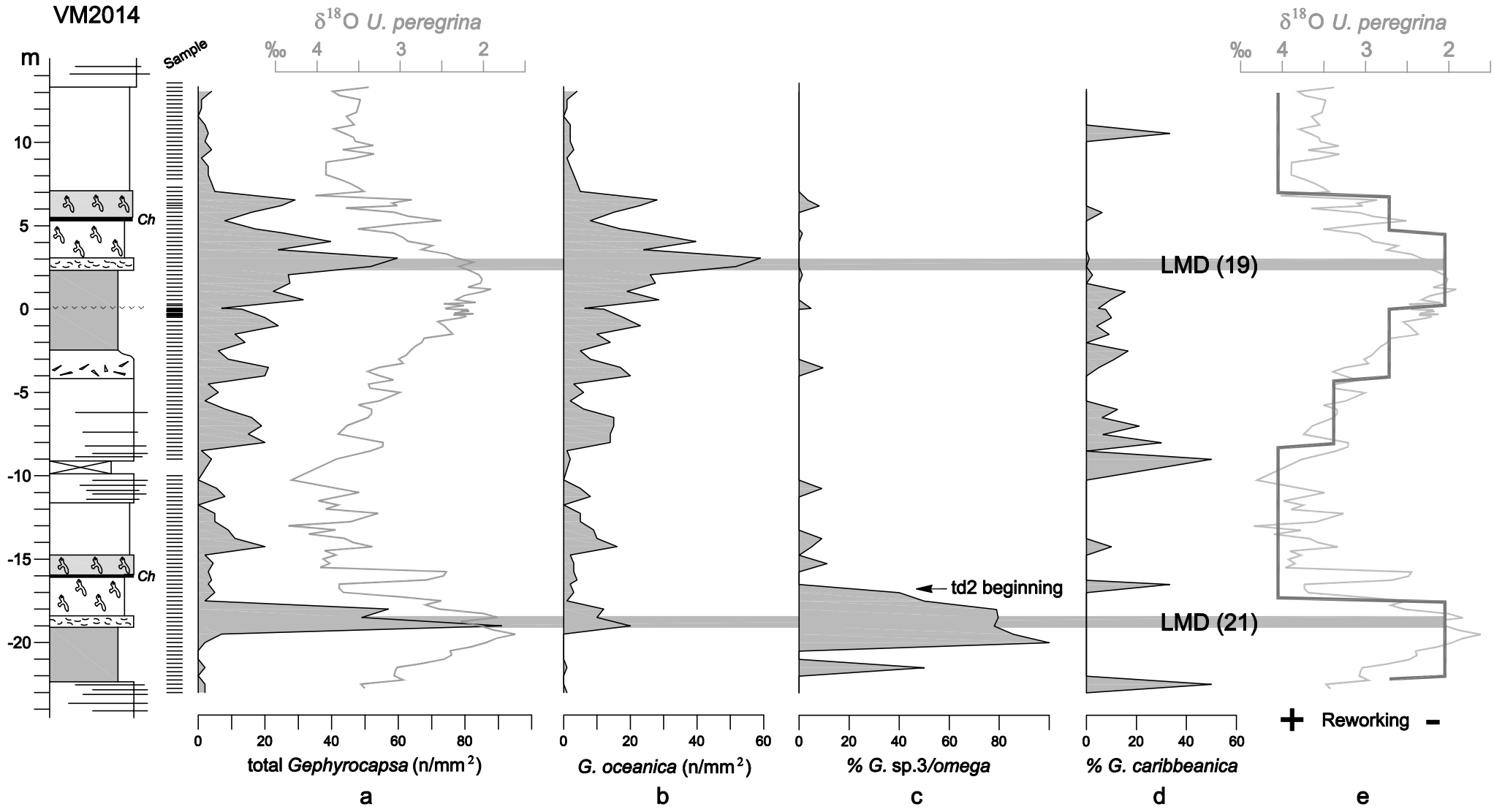
VM2014
m
Sample
Ch
Ch
10
5
0
-5
-10
-15
-20
δ18O U. peregrina
‰ 4 3 2
LMD (19)
LMD (21)
td2 beginning
0 20 40 60 80
total Gephyrocapsa (n/mm2)
a
0 20 40 60
G. oceanica (n/mm2)
b
0 20 40 60 80
% G. sp.3/omega
c
0 20 40 60
% G. caribbeanica
d
δ18O U. peregrina
‰ 4 3 2
+ Reworking -
e

Figure 7

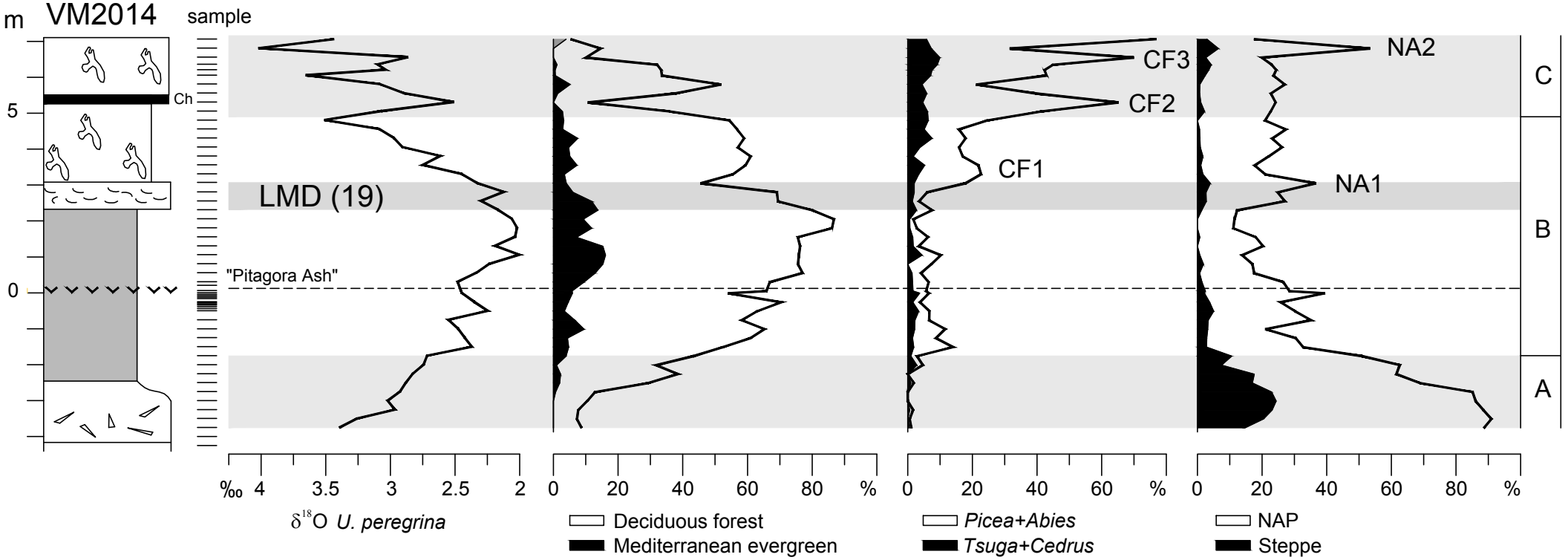
m
VM2014
sample
Ch
5
0
LMD (19)
"Pitagora Ash"
CF3
CF2
CF1
NA2
NA1
C
B
A
‰ 4 3.5 3 2.5 2
δ18O U. peregrina
0 20 40 60 80 %
Deciduous forest
Mediterranean evergreen
0 20 40 60 %
Picea+Abies
Tsuga+Cedrus
0 20 40 60 80 %
NAP
Steppe

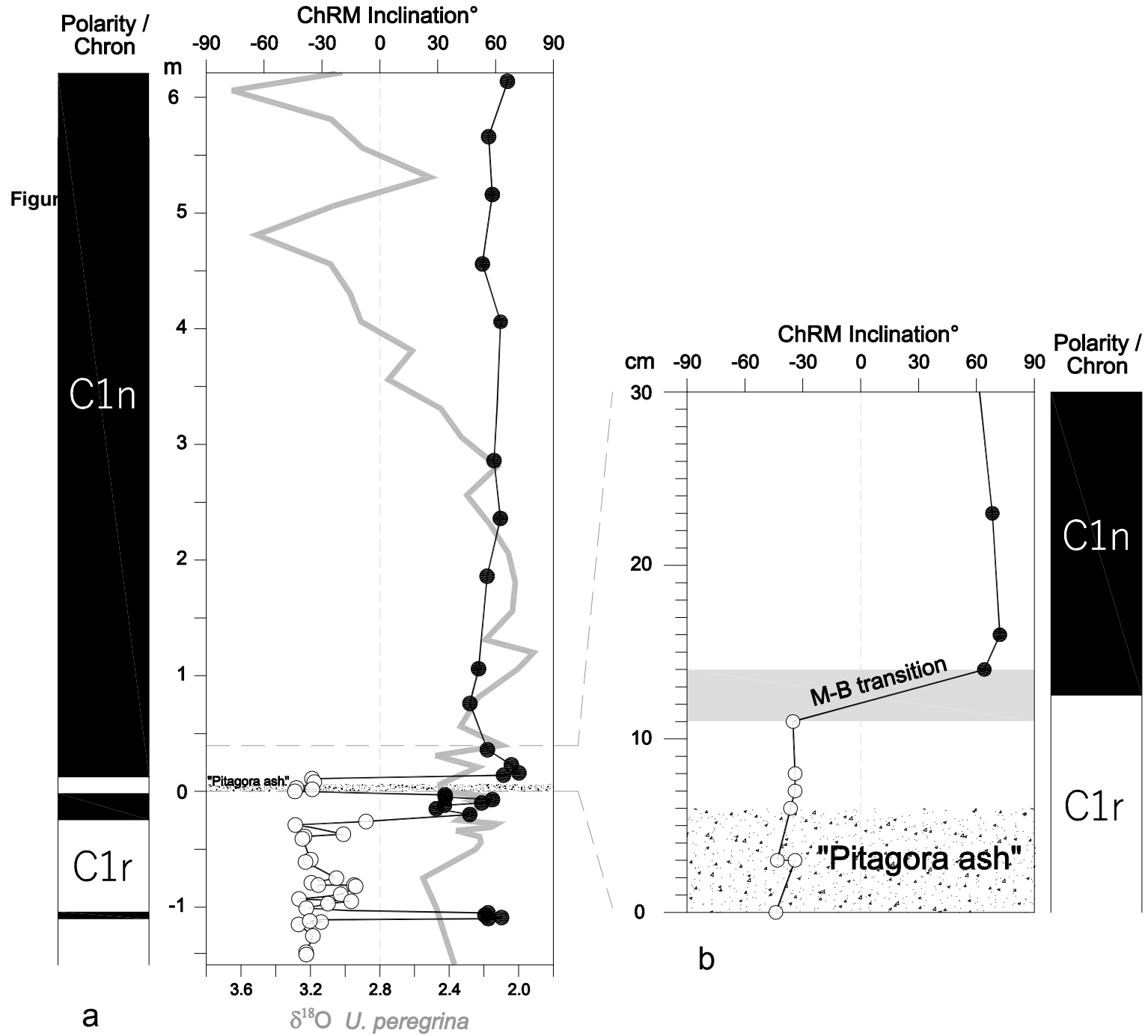
Polarity / Chron
ChRM Inclination°
-90 -60 -30 0 30 60 90
m
6
5
4
3
2
1
0
-1
C1n
C1r
"Pitagora ash"
3.6 3.2 2.8 2.4 2.0
δ18O U. peregrina
a
cm
30
20
10
0
M-B transition
"Pitagora ash"
b